Linear-response functions of molecules on a quantum computer: Charge and spin responses and optical absorption

Taichi Kosugi and Yu-ichiro Matsushita

Laboratory for Materials and Structures, Institute of Innovative Research, Tokyo Institute of Technology, Yokohama 226-8503, Japan and Quemix Inc., Taiyo Life Nihombashi Building, 2-11-2, Nihombashi Chuo-ku, Tokyo 103-0027, Japan

(Received 17 January 2020; revised 27 January 2020; accepted 22 May 2020; published 9 July 2020)

We propose a scheme for the construction of linear-response functions of an interacting electronic system via quantum phase estimation and statistical sampling on a quantum computer. By using the unitary decomposition of electronic operators for avoiding the difficulty due to their nonunitarity, we provide the circuits equipped with ancillae for probabilistic preparation of qubit states on which the necessary nonunitary operators have acted. We perform simulations of such construction of the charge and spin response functions and photoabsorption cross sections for C_2 and N_2 molecules by comparing with the results from full configuration-interaction calculations. It is found that the accurate detection of subtle structures coming from the weak poles in the response functions requires a large number of measurements.

DOI: 10.1103/PhysRevResearch.2.033043

I. INTRODUCTION

Since the information carrier of a programmable quantum computer is a set of qubits that exploits the principle of superposition, essentially parallel algorithms can exist and perform computation for classically formidable problems [1,2]. Quantum chemistry [3] is believed to be one of the most suitable research fields for quantum computation since its problem setting is quantum mechanical by definition. Indeed, a quantum computer can treat a many-electron state composed of lots of Slater determinants as it is in a sense that the electronic state is encoded as a superposition of qubit states via an appropriately chosen map such as the Jordan–Wigner (JW) [4] and Bravyi–Kitaev (BK) [5] transformations.

The quantity which a quantum chemistry calculation is asked to first provide is the total energy of a target system [6]. One of the most widespread methods for obtaining the total energy is the variational quantum eigensolver (VQE), in which a trial many-electron state is prepared via a parametrized quantum circuit. The parameters are optimized iteratively with the aid of a classical computer aiming at the ground state. This approach was first realized [7] by using a quantum photonic device, after which the realizations by superconducting [8,9] and ion trap [10] quantum computers have been reported. There exist algorithms for obtaining the energy spectra of excited states [11–16].

Not only academic interest but also industrial demands for accurate explanations and predictions of material properties make it an urgent task to develop methodologies on quantum computers for various electronic properties other than energy levels. The one-particle Green's functions (GFs) are important in correlated electronic systems [17,18] since they are often used in explanation of spectra measured in photoemission and its inverse experiments. Recently we proposed [19] a method for the GFs [20,21] via statistical sampling by employing quantum phase estimation (QPE) [1]. Endo *et al.* [22], on the other hand, proposed a method for the GFs by focusing on noisy intermediate-scale quantum (NISQ) devices.

The charge and spin response functions, formulated in the linear-response theory [23,24], describe the leading contributions to the electric and magnetic excitations when perturbation fields are applied to a target system. Since the response functions are the fundamental building blocks in constructing the elaborated methods for correlated electrons such as *GW* theory [23,25], the accurate calculation of them is needed. In addition, there exist response functions directly related to measurable quantities such as dielectric constants, electric conductivities, and magnetic susceptibilities.

Given the recent rapid development of fabrication techniques for quantum hardware and the growing demands for quantum computation in material science, it is worth making tools for analyses on correlation effects. In this study, we propose a scheme for the construction of the response functions of an interacting electronic system via statistical sampling on a quantum computer. We track the changes in the state of qubits analytically when they undergo gate operations and measurements to derive the exact probability distributions of the outcomes. For examining the validity of our scheme, we perform the full configuration-interaction (FCI) calculations for diatomic molecules, from which we simulate the measurements on qubits to get the response functions by generating random numbers based on the exact probability distributions.

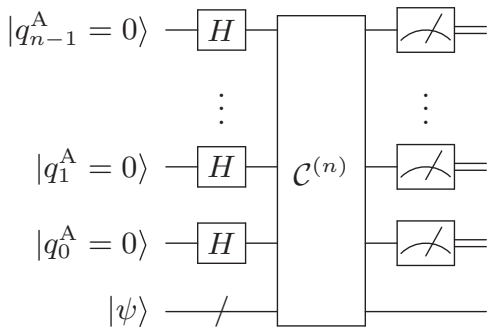

FIG. 1. Circuit $\mathcal{C}_{\mathcal{O}}$ for the probabilistic preparation of a state on which a linear combination $\mathcal{O}$ of 2^n unitaries has acted. H in the circuit represents the Hadamard gate. The desired state is prepared according to a measurement outcome of n ancillary qubits. This circuit contains $\mathcal{C}^{(n)}$ as a partial circuit defined in Fig. 2.

This paper is organized as follows. In Sec. II, we explain the basic ideas and our scheme in detail by providing the quantum circuits for obtaining the response functions via statistical sampling. In Sec. III, we describe the computational details for our simulations on a classical computer. In Sec. IV, we show the simulation results for C_2 and N_2 molecules. In Sec. V, we provide the conclusions.

II. METHODS

A. Circuit for a linear combination of unitaries

The calculation of a physical quantities of interest quite often involves the evaluation of matrix elements of various electronic operators. Such an operator is, however, not necessarily unitary and it prohibits one from implementing it straightforwardly as logic gates for qubits. We describe a workaround for this difficulty by providing a circuit for probabilistic state preparation.

For 2^n unitaries U_k, where k is a bit string of length n, we want to apply an arbitrary linear combination of them,

$$\mathcal{O} = c_{0\cdots00}U_{0\cdots00} + c_{0\cdots01}U_{0\cdots01} + \cdots + c_{1\cdots11}U_{1\cdots11}, \quad (1)$$

to an input register $|\psi\rangle$. $c_k \equiv |c_k|\exp(i\phi_k)$ is the complex coefficient. We construct a circuit $\mathcal{C}_{\mathcal{O}}$ equipped with n ancillary qubits, as depicted in Fig. 1, containing a partial circuit $\mathcal{C}^{(n)}$ defined recursively in Fig. 2. If the measurement outcome for the ancillae is $|0\rangle^{\otimes n}$, the state of the whole system collapses to $|0\rangle^{\otimes n} \otimes \mathcal{O}|\psi\rangle$ up to a normalization constant. The proof of this fact is provided in Appendix A.

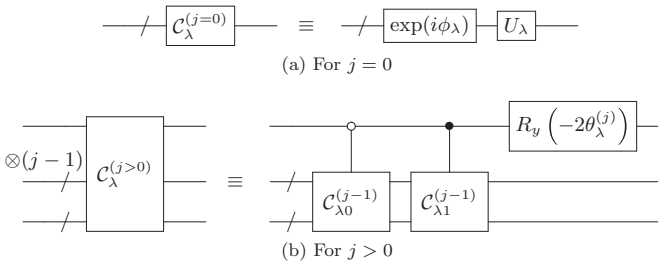

FIG. 2. Recursive definitions of circuits $\mathcal{C}^{(j)}_{\lambda}$ for (a) $j=0$ and (b) $j>0$. λ is empty or a bit string. $\exp(i\phi_\lambda)$ is an identity operator multiplied by the phase factor. $R_y(\theta) = e^{-i\theta\sigma_y/2}$ is a rotation for an angle θ. These circuits are used in Fig. 1.

The state preparation techniques for the response functions described below are special cases of the one introduced above with some target-specific modifications.

B. Definitions for linear responses

1. Linear-response functions

We work with the n_{orbs} orthonormalized spatial one-electron orbitals for each spin direction in a target N-electron system, which we assume is in the many-electron ground state $|\Psi_{\mathrm{gs}}\rangle$ at zero temperature. The formalism described below can be easily extended to a system with multiple ground states and/or a nonzero temperature.

The response functions in terms of Hermitian operators $\mathcal{O}$ and $\mathcal{O}'$ in time domain is defined as [23]

$$\chi_{\mathcal{O}\mathcal{O}'}(t,t') \equiv -i\theta(t-t')\langle[\mathcal{O}(t),\mathcal{O}'(t')]\rangle, \quad (2)$$

where $\mathcal{O}(t)$ is the operator in the Heisenberg picture and the expectation value is for the ground state. We assume that the system has been in the equilibrium when the perturbation is turned on. Since the response function defined in Eq. (2) depends on time only via $t-t'$ in this case, its expression in frequency domain is written as

$$\chi_{\mathcal{O}\mathcal{O}'}(\omega) = R_{\mathcal{O}\mathcal{O}'}(\omega+i\delta) + R_{\mathcal{O}'\mathcal{O}}(-\omega-i\delta), \quad (3)$$

for a real frequency ω.

$$R_{\mathcal{O}\mathcal{O}'}(z) \equiv \sum_{\lambda} \frac{L_{\lambda\mathcal{O}\mathcal{O}'}}{z-\left(E_\lambda - E^N_{\mathrm{gs}}\right)} \quad (4)$$

is the Lehmann summation over the energy eigenstates for a complex frequency z. E^N_{gs} is the ground-state energy and E_λ is the energy eigenvalue of the λth excited state $|\Psi_\lambda\rangle$.

$$L_{\lambda\mathcal{O}\mathcal{O}'} \equiv \langle\Psi_{\mathrm{gs}}|\mathcal{O}|\Psi_\lambda\rangle\langle\Psi_\lambda|\mathcal{O}'|\Psi_{\mathrm{gs}}\rangle \quad (5)$$

is the transition matrix element, which satisfies clearly $L_{\lambda\mathcal{O}\mathcal{O}'} = (L_{\lambda\mathcal{O}'\mathcal{O}})^*$. The positive infinitesimal constant δ appears in Eq. (3) due to the retarded nature of the response function, rendering all the poles immediately below the real axis. It is clear that the real part of $\chi_{\mathcal{O}\mathcal{O}'}(\omega)$ is even with respect to ω, while the imaginary part is odd.

2. Charge and spin responses

By using the creation $a^\dagger_{p\sigma}$ and annihilation $a_{p\sigma}$ operators for the pth spatial orbital of σ spin $|\phi_{p\sigma}\rangle$ ($\sigma = \alpha, \beta$), the electron number operator is given by $n_{p\sigma} = a^\dagger_{p\sigma}a_{p\sigma}$. The spin operator is given by $\boldsymbol{s}_p = \sum_{\sigma,\sigma'} a^\dagger_{p\sigma}(\boldsymbol{\sigma}^{\mathrm{el}}_{\sigma\sigma'}/2)a_{p\sigma'}$, where $\boldsymbol{\sigma}^{\mathrm{el}}$ is the Pauli matrix for the electronic state.

The orbital-wise response functions involving the charge and spin of the individual spin orbitals are obtained by putting $\mathcal{O}_{pn} \equiv \sum_\sigma n_{p\sigma}$ and $\mathcal{O}_{pj} \equiv s_{pj}$ ($j = x, y, z$), respectively, into Eq. (4). To rewrite the expression for transition matrix elements in Eq. (5) into a more tractable form, we define the charge-charge transition matrix element,

$$N_{\lambda p\sigma,p'\sigma'} \equiv \langle\Psi_{\mathrm{gs}}|n_{p\sigma}|\Psi_\lambda\rangle\langle\Psi_\lambda|n_{p'\sigma'}|\Psi_{\mathrm{gs}}\rangle, \quad (6)$$

for the λth energy eigenstate $|\Psi_\lambda\rangle$ of the N-electron states. We define similarly the spin-spin one,

$$S_{\lambda pj,p'j'} \equiv \langle\Psi_{\rm gs}|s_{pj}|\Psi_\lambda\rangle\langle\Psi_\lambda|s_{p'j'}|\Psi_{\rm gs}\rangle, \tag{7}$$

for $j, j' = x, y, z$ and the spin-charge one,

$$M_{\lambda pj,p'\sigma'} \equiv \langle\Psi_{\rm gs}|s_{pj}|\Psi_\lambda\rangle\langle\Psi_\lambda|n_{p'\sigma'}|\Psi_{\rm gs}\rangle \equiv M^*_{\lambda p'\sigma',pj}. \tag{8}$$

From these matrix elements, we define the following Hermitian matrices L_λ:

$$L_{\lambda pn,p'n} \equiv \sum_{\sigma,\sigma'} N_{\lambda p\sigma,p'\sigma'}, \tag{9}$$

$$L_{\lambda pj,p'j'} \equiv S_{\lambda pj,p'j'}, \tag{10}$$

$$L_{\lambda pj,p'n} \equiv \sum_{\sigma} M_{\lambda pj,p'\sigma}, \tag{11}$$

which are used for Eq. (5).

3. Generic one-body operators

A generic one-body operator is given in the form,

$$\mathcal{O} = \sum_{m,m'} \mathcal{O}_{mm'} a^\dagger_m a_{m'}, \tag{12}$$

where m and m' are the composite indices of spatial orbitals and spins. $\mathcal{O}_{mm'}$ is the matrix element between the one-electron orbitals. Our scheme is actually applicable to such a generic case for $\mathcal{O}$ and $\mathcal{O}'$, for which we have to obtain the transition matrix elements,

$$B_{\lambda m_1 m_2,m_3 m_4} \equiv \langle\Psi_{\rm gs}|a^\dagger_{m_1} a_{m_2}|\Psi_\lambda\rangle\langle\Psi_\lambda|a^\dagger_{m_3} a_{m_4}|\Psi_{\rm gs}\rangle, \tag{13}$$

which satisfy clearly $B_{\lambda m_1 m_2,m_3 m_4} = (B_{\lambda m_4 m_3,m_2 m_1})^*$. From them, we sum up the contributions to Eq. (5) as

$$L_{\lambda\mathcal{O}\mathcal{O}'} = \sum_{m_1,m_2,m_3,m_4} \mathcal{O}_{m_1 m_2} \mathcal{O}'_{m_3 m_4} B_{\lambda m_1 m_2,m_3 m_4}. \tag{14}$$

We calculate the electric polarizabilities of molecules in the present study as examples for the generic scheme. The contribution from electrons to the electric dipole of a molecule is $\boldsymbol{d} = -\sum_{m,m'} \boldsymbol{d}_{mm'} a^\dagger_m a_{m'}$, where the negative sign on the right-hand side comes from the electron charge. $\boldsymbol{d}_{mm'} \equiv \langle\phi_m|\boldsymbol{r}|\phi_{m'}\rangle$ is the matrix element of position operator. The linear electric polarizability tensor $\alpha_{jj'}$ ($j, j' = x, y, z$) [26,27] is defined as the first derivative of the expected electric dipole with respect to an external electric field, obtained via the response function as $\alpha_{jj'}(\omega) = -\chi_{d_j d_{j'}}(\omega)$, from which the photoabsorption cross section [28] is given by

$$\sigma(\omega) = \frac{4\pi}{c}\omega \mathrm{Im}\mathrm{Tr}\,\alpha(\omega). \tag{15}$$

This cross section is a measurable quantity in optical absorption experiments.

4. Unitary decomposition of electronic operators

Although there are alternatives for mapping the electronic operators of a target system to the qubit ones such as JW [4] and BK [5] transformations, we do not distinguish between an electronic operator and its corresponding qubit representation in what follows since no confusion will occur for the readers.

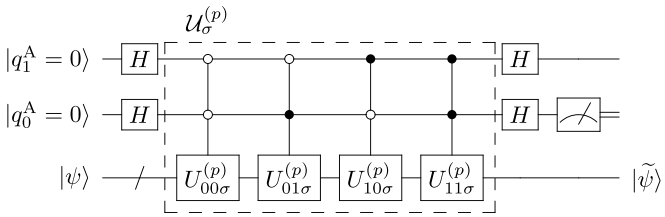

FIG. 3. Charge-charge diagonal circuit $\mathcal{C}_{p\sigma}$ ($\sigma = \alpha, \beta$) for probabilistic preparation of $n_{p\sigma}|\psi\rangle$ and $\widetilde{n}_{p\sigma}|\psi\rangle$ from an arbitrary input state $|\psi\rangle$ and two ancillary qubits. We define the partial circuit $\mathcal{U}_\sigma^{(p)}$ by enclosing it with dashed lines.

For each combination of a spatial orbital p and a spin σ, we perform the Majorana fermion-like [29] transformation for the qubits [19]:

$$U_{0p\sigma} = a_{p\sigma} + a^\dagger_{p\sigma}, \tag{16}$$

and

$$U_{1p\sigma} = a_{p\sigma} - a^\dagger_{p\sigma}, \tag{17}$$

which are unitary regardless of the adopted qubit representation thanks to the anticommutation relation between the electronic operators and can thus be implemented as logic gates in the quantum computer. This means that we can prepare at least probabilistically an electronic state on which an arbitrary product of the creation and annihilation operators has acted, similarly to the case for GFs [19].

In what follows, we assume that the many-electron ground state $|\Psi_{\rm gs}\rangle$ is already known and can be prepared on a quantum computer.

C. Charge-charge responses

Let us first consider the determination of the charge-charge transition matrices N_λ.

1. Circuits for diagonal components

From the unitary operators in Eqs. (16) and (17) for a combination of a spatial orbital p and a spin σ, we define $U^{(p)}_{\kappa\kappa'\sigma} \equiv U_{\kappa p\sigma} U_{\kappa' p\sigma}$ for $\kappa, \kappa' = 0, 1$, which are also unitary. With them, the electron number operator is written as

$$n_{p\sigma} = \frac{U^{(p)}_{00\sigma} + U^{(p)}_{01\sigma} - U^{(p)}_{10\sigma} - U^{(p)}_{11\sigma}}{4}, \tag{18}$$

while the whole number operator is written as

$$\widetilde{n}_{p\sigma} \equiv 1 - n_{p\sigma} = \frac{U^{(p)}_{00\sigma} - U^{(p)}_{01\sigma} + U^{(p)}_{10\sigma} - U^{(p)}_{11\sigma}}{4}. \tag{19}$$

We construct a circuit $\mathcal{C}_{p\sigma}$ equipped with two ancillary qubits $|q_0^{\rm A}\rangle$ and $|q_1^{\rm A}\rangle$ by implementing the controlled operations of $U^{(p)}_{\kappa\kappa'\sigma}$, as depicted in Fig. 3. The whole system consists of the ancillae and an arbitrary input register $|\psi\rangle$. Its state changes by undergoing the circuit as

$$\begin{aligned} &\left|q_1^{\rm A}=0\right\rangle \otimes \left|q_0^{\rm A}=0\right\rangle \otimes |\psi\rangle \\ &\longmapsto |0\rangle \otimes |1\rangle \otimes \widetilde{n}_{p\sigma}|\psi\rangle + |1\rangle \otimes |0\rangle \otimes n_{p\sigma}|\psi\rangle \equiv |\Phi_{p\sigma}\rangle, \end{aligned} \tag{20}$$

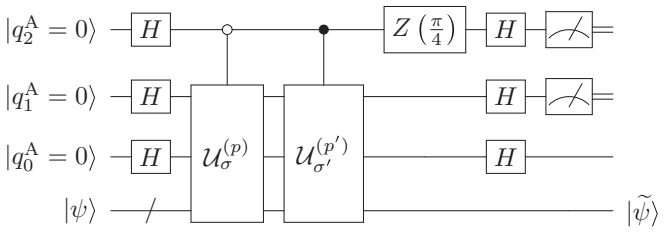

FIG. 4. Charge-charge off-diagonal circuit $\mathcal{C}_{p\sigma,p'\sigma'}$ ($\sigma,\sigma'=\alpha,\beta$) for probabilistic preparation of $n^{\pm}_{p\sigma,p'\sigma'}|\psi\rangle$ and $\widetilde{n}^{\pm}_{p\sigma,p'\sigma'}|\psi\rangle$ from an arbitrary input state $|\psi\rangle$ and three ancillary qubits. $Z(\pm\pi/4)=\mathrm{diag}(1,e^{\pm i\pi/4})$ is a phase gate. The partial circuits defined in Fig. 3 are contained as the controlled subroutines.

since $(a^\dagger_{p\sigma})^2$ and $a^2_{p\sigma}$ vanish due to the Fermi statistics. The projective measurement [1] on $|q_0^{\rm A}\rangle$ is represented by the two operators $\mathcal{P}_q=I\otimes|q\rangle\langle q|\otimes I$ ($q=0,1$). The state of the whole system collapses immediately after the measurement as follows:

$$|\Phi_{p\sigma}\rangle \overset{|0\rangle\ \text{observed}}{\longmapsto} |1\rangle\otimes|0\rangle\otimes\frac{n_{p\sigma}}{\sqrt{\mathbb{P}_{p\sigma}}}|\psi\rangle,$$
$$\text{prob.}\ \|n_{p\sigma}|\psi\rangle\|^2\equiv\mathbb{P}_{p\sigma}, \tag{21}$$
$$|\Phi_{p\sigma}\rangle \overset{|1\rangle\ \text{observed}}{\longmapsto} |0\rangle\otimes|1\rangle\otimes\frac{\widetilde{n}_{p\sigma}}{\sqrt{\widetilde{\mathbb{P}}_{p\sigma}}}|\psi\rangle,$$
$$\text{prob.}\ \|\widetilde{n}_{p\sigma}|\psi\rangle\|^2\equiv\widetilde{\mathbb{P}}_{p\sigma}. \tag{22}$$

2. Circuits for off-diagonal components

For mutually different combinations (p,σ) and (p',σ') of spatial orbitals and spins, we define the four non-Hermitian auxiliary operators,

$$n^{\pm}_{p\sigma,p'\sigma'}\equiv\frac{n_{p\sigma}\pm e^{i\pi/4}n_{p'\sigma'}}{2}, \tag{23}$$

and

$$\widetilde{n}^{\pm}_{p\sigma,p'\sigma'}\equiv\frac{\widetilde{n}_{p\sigma}\pm e^{i\pi/4}\widetilde{n}_{p'\sigma'}}{2}. \tag{24}$$

Un-normalized auxiliary states $|\Psi^{\pm}_{p\sigma,p'\sigma'}\rangle\equiv n^{\pm}_{p\sigma,p'\sigma'}|\Psi_{\rm gs}\rangle$ can have overlaps $T^{\pm}_{\lambda p\sigma,p'\sigma'}\equiv|\langle\Psi_\lambda|\Psi^{\pm}_{p\sigma,p'\sigma'}\rangle|^2$ with the energy eigenstates, from which the charge-charge transition matrix elements in Eq. (6) can be calculated as

$$N_{\lambda p\sigma,p'\sigma'}=e^{-i\pi/4}(T^{+}_{\lambda p\sigma,p'\sigma'}-T^{-}_{\lambda p\sigma,p'\sigma'})+e^{i\pi/4}(T^{+}_{\lambda p'\sigma',p\sigma}-T^{-}_{\lambda p'\sigma',p\sigma}). \tag{25}$$

We construct a circuit $\mathcal{C}_{p\sigma,p'\sigma'}$ equipped with three ancillary qubits by using the controlled operations of the partial circuits $\mathcal{U}_\sigma^{(p)}$ and $\mathcal{U}_{\sigma'}^{(p')}$, defined in Fig. 3, as depicted in Fig. 4. The whole system consists of the ancillae and an arbitrary input register $|\psi\rangle$. Its state changes by undergoing the circuit as

$$\begin{aligned}|q_2^{\rm A}=0\rangle\otimes|q_1^{\rm A}=0\rangle\otimes|q_0^{\rm A}=0\rangle\otimes|\psi\rangle&\\ \longmapsto|0\rangle\otimes|0\rangle\otimes|1\rangle\otimes\widetilde{n}^{+}_{p\sigma,p'\sigma'}|\psi\rangle&\\ +|0\rangle\otimes|1\rangle\otimes|0\rangle\otimes n^{+}_{p\sigma,p'\sigma'}|\psi\rangle&\\ +|1\rangle\otimes|0\rangle\otimes|1\rangle\otimes\widetilde{n}^{-}_{p\sigma,p'\sigma'}|\psi\rangle&\\ +|1\rangle\otimes|1\rangle\otimes|0\rangle\otimes n^{-}_{p\sigma,p'\sigma'}|\psi\rangle&\\ \equiv|\Phi_{p\sigma,p'\sigma'}\rangle.&\end{aligned} \tag{26}$$

The projective measurement on $|q_2^{\rm A}\rangle$ and $|q_1^{\rm A}\rangle$ is represented by the four operators $\mathcal{P}_{qq'}=|q\rangle\langle q|\otimes|q'\rangle\langle q'|\otimes I\otimes I$ ($q,q'=0,1$). The two outcomes among the possible four are of our interest, immediately after which the whole system collapses as follows:

$$|\Phi_{p\sigma,p'\sigma'}\rangle \overset{|0\rangle\otimes|1\rangle\ \text{observed}}{\longmapsto} |0\rangle\otimes|1\rangle\otimes|0\rangle\otimes\frac{n^{+}_{p\sigma,p'\sigma'}}{\sqrt{\mathbb{P}^{+}_{p\sigma,p'\sigma'}}}|\psi\rangle,$$
$$\text{prob.}\ \|n^{+}_{p\sigma,p'\sigma'}|\psi\rangle\|^2\equiv\mathbb{P}^{+}_{p\sigma,p'\sigma'}, \tag{27}$$
$$|\Phi_{p\sigma,p'\sigma'}\rangle \overset{|1\rangle\otimes|1\rangle\ \text{observed}}{\longmapsto} |1\rangle\otimes|1\rangle\otimes|0\rangle\otimes\frac{n^{-}_{p\sigma,p'\sigma'}}{\sqrt{\mathbb{P}^{-}_{p\sigma,p'\sigma'}}}|\psi\rangle,$$
$$\text{prob.}\ \|n^{-}_{p\sigma,p'\sigma'}|\psi\rangle\|^2\equiv\mathbb{P}^{-}_{p\sigma,p'\sigma'}. \tag{28}$$

3. Transition matrices via statistical sampling

Given the result of a measurement on the ancillary bits for a diagonal or an off-diagonal component, we have the register $|\widetilde{\psi}\rangle$ different from the input N-electron state. Then we perform QPE for the Hamiltonian $\mathcal{H}$ by inputting $|\widetilde{\psi}\rangle$ to obtain one of the energy eigenvalues in the Hilbert subspace for the N-electron states. A QPE experiment inevitably suffers from probabilistic errors that depend on the number of qubits and the various parameters for the Suzuki-Trotter decomposition of $\mathcal{H}$. We assume for simplicity, however, that the QPE procedure is realized on a quantum computer with ideal precision as well as in our previous study [19]. We will thus find the estimated value to be E^N_λ with a probability $|\langle\Psi_\lambda|\widetilde{\psi}\rangle|^2$ [1]. Since the probabilistic state preparation and obtaining the transition matrix elements are dominated mathematically by multinomial distributions, the errors in the response function scale as $N_{\rm meas}^{-1/2}$ for $N_{\rm meas}$ repeated measurements.

If we input $|\Psi_{\rm gs}\rangle$ to the diagonal circuit $\mathcal{C}_{p\sigma}$ in Fig. 3 and observe the ancillary bit $|q_0^{\rm A}=0\rangle$ for QPE, the energy eigenvalue E^N_λ will be obtained with a probability [see Eq. (21)],

$$\left|\langle\Psi_\lambda|\frac{n_{p\sigma}}{\sqrt{\mathbb{P}_{p\sigma}}}|\Psi_{\rm gs}\rangle\right|^2\mathbb{P}_{p\sigma}=N_{\lambda p\sigma,p\sigma}. \tag{29}$$

This means that we can get the diagonal components of transition matrices N_λ via statistical sampling for a fixed combination of p and σ.

If we input $|\Psi_{\rm gs}\rangle$ to the off-diagonal circuit $\mathcal{C}_{p\sigma,p'm'}$ in Fig. 4 and observe the ancillary bits $|q_2^{\rm A}=0\rangle\otimes|q_1^{\rm A}=1\rangle$ or $|q_2^{\rm A}=1\rangle\otimes|q_1^{\rm A}=1\rangle$ for QPE, the energy eigenvalue E^N_λ will be obtained with probabilities [see Eqs. (27) and (28)],

$$\left|\langle\Psi_\lambda|\frac{n^{\pm}_{p\sigma,p'\sigma'}}{\sqrt{\mathbb{P}^{\pm}_{p\sigma,p'\sigma'}}}|\Psi_{\rm gs}\rangle\right|^2\mathbb{P}^{\pm}_{p\sigma,p'\sigma'}=T^{\pm}_{\lambda p\sigma,p'\sigma'}. \tag{30}$$

This means that we can get the off-diagonal components of N_λ from Eq. (25) via statistical sampling for a fixed combination of p, p', σ, and σ'.

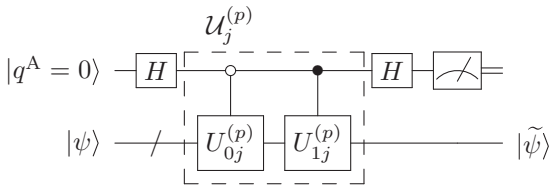

FIG. 5. Spin-spin diagonal circuit $\mathcal{C}_{pj}$ $(j=x,y)$ for probabilistic preparation of $s_{pj}|\psi\rangle$ and $\widetilde{s}_{pj}|\psi\rangle$ from an arbitrary input state $|\psi\rangle$ and an ancillary qubit. We define the partial circuit $\mathcal{U}_j^{(p)}$ by enclosing it with dashed lines.

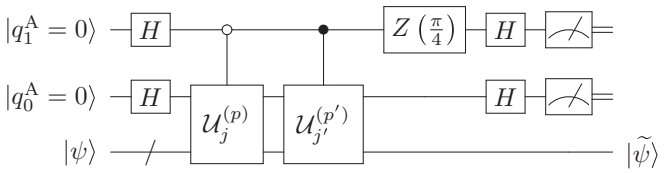

FIG. 6. Spin-spin off-diagonal circuit $\mathcal{C}_{pj,p'j'}$ $(j,j'=x,y)$ for probabilistic preparation of $s^{\pm}_{pj,p'j'}|\psi\rangle$ and $\widetilde{s}^{\pm}_{pj,p'j'}|\psi\rangle$ from an arbitrary input state $|\psi\rangle$ and two ancillary qubits. The partial circuits defined in Fig. 5 are contained as the controlled subroutines.

D. Spin-spin responses

Let us next consider the determination of the spin-spin transition matrix elements $S_{\lambda pj,p'j'}$ for $j,j'=x,y$. Since the operators of the z component of spin and the electron number are related via $s_{pz}=(n_{p\alpha}-n_{p\beta})/2$, the matrix elements $S_{\lambda pz,p'z}$ can be calculated from the diagonal and off-diagonal components of N_λ, already obtained in Sec. II C. $S_{\lambda pj,p'z}$ can be calculated from M_λ which will be explained in Sec. II E.

1. Circuits for diagonal components

From the unitary operators in Eqs. (16) and (17) for a combination of a spatial orbital p and a spin σ, we define the following four unitary operators: $U_{0x}^{(p)}\equiv U_{0p\alpha}U_{1p\beta}$, $U_{1x}^{(p)}\equiv -U_{1p\alpha}U_{0p\beta}$, $U_{0y}^{(p)}\equiv -iU_{0p\alpha}U_{0p\beta}$, and $U_{1y}^{(p)}\equiv iU_{1p\alpha}U_{1p\beta}$. With them, the spin operators for the x and y directions are written as

$$s_{pj}=\frac{U_{0j}^{(p)}+U_{1j}^{(p)}}{4} \tag{31}$$

for $j=x,y$. We define

$$\widetilde{s}_{pj}\equiv\frac{U_{0j}^{(p)}-U_{1j}^{(p)}}{4} \tag{32}$$

for later convenience.

We construct a circuit $\mathcal{C}_{pj}$ equipped with an ancillary qubit by implementing the controlled operations of $U_{0j}^{(p)}$ and $U_{1j}^{(p)}$, as depicted in Fig. 5. The whole system consists of the ancilla and an arbitrary input register $|\psi\rangle$. Its state changes by undergoing the circuit as

$$\begin{aligned}|q^{\rm A}=0\rangle\otimes|\psi\rangle &\longmapsto |0\rangle\otimes 2s_{pj}|\psi\rangle+|1\rangle\otimes 2\widetilde{s}_{pj}|\psi\rangle\\ &\equiv|\Phi_{pj}\rangle.\end{aligned} \tag{33}$$

The projective measurement on $|q^{\rm A}\rangle$ is represented by the two operators $\mathcal{P}_q=|q\rangle\langle q|\otimes I$ $(q=0,1)$. The state of the whole system collapses immediately after the measurement as follows:

$$\begin{aligned}|\Phi_{pj}\rangle &\overset{|0\rangle\ \text{observed}}{\longmapsto} |0\rangle\otimes\frac{2s_{pj}}{\sqrt{\mathbb{P}_{pj}}}|\psi\rangle,\\ \text{prob. }\|2s_{pj}|\psi\rangle\|^2 &\equiv\mathbb{P}_{pj},\\ |\Phi_{pj}\rangle &\overset{|1\rangle\ \text{observed}}{\longmapsto} |1\rangle\otimes\frac{2\widetilde{s}_{pj}}{\sqrt{\widetilde{\mathbb{P}}_{pj}}}|\psi\rangle,\\ \text{prob. }\|2\widetilde{s}_{pj}|\psi\rangle\|^2 &\equiv\widetilde{\mathbb{P}}_{pj}.\end{aligned} \tag{34, 35}$$

2. Circuits for off-diagonal components

For mutually different combinations (p,j) and (p',j') of spatial orbitals and spin components $j,j'=x,y$, we define the four non-Hermitian auxiliary operators,

$$s^{\pm}_{pj,p'j'}\equiv\frac{s_{pj}\pm e^{i\pi/4}s_{p'j'}}{2}, \tag{36}$$

and

$$\widetilde{s}^{\pm}_{pj,p'j'}\equiv\frac{\widetilde{s}_{pj}\pm e^{i\pi/4}\widetilde{s}_{p'j'}}{2}. \tag{37}$$

Un-normalized auxiliary states $|\Psi^{\pm}_{pj,p'j'}\rangle\equiv s^{\pm}_{pj,p'j'}|\Psi_{\rm gs}\rangle$ can have overlaps $T^{\pm}_{\lambda pj,p'j'}\equiv|\langle\Psi_\lambda|\Psi^{\pm}_{pj,p'j'}\rangle|^2$ with the energy eigenstates, from which the spin-spin transition matrix elements in Eq. (7) can be calculated as

$$\begin{aligned}S_{\lambda pj,p'j'}=\ &e^{-i\pi/4}(T^{+}_{\lambda pj,p'j'}-T^{-}_{\lambda pj,p'j'})\\ &+e^{i\pi/4}(T^{+}_{\lambda p'j',pj}-T^{-}_{\lambda p'j',pj}).\end{aligned} \tag{38}$$

We construct a circuit $\mathcal{C}_{pj,p'j'}$ equipped with two ancillary qubits by using the controlled operations of the partial circuits $\mathcal{U}_j^{(p)}$ and $\mathcal{U}_{j'}^{(p')}$, defined in Fig. 5, as depicted in Fig. 6. The whole system consists of the ancillae and an arbitrary input register $|\psi\rangle$. Its state changes by undergoing the circuit as

$$\begin{aligned}|q_1^{\rm A}\ &=\ 0\rangle\otimes|q_0^{\rm A}=0\rangle\otimes|\psi\rangle\\ &\longmapsto |0\rangle\otimes|0\rangle\otimes 2s^{+}_{pj,p'j'}|\psi\rangle+|0\rangle\otimes|1\rangle\otimes 2\widetilde{s}^{+}_{pj,p'j'}|\psi\rangle\\ &\quad+|1\rangle\otimes|0\rangle\otimes 2s^{-}_{pj,p'j'}|\psi\rangle+|1\rangle\otimes|1\rangle\otimes 2\widetilde{s}^{-}_{pj,p'j'}|\psi\rangle\\ &\equiv\ |\Phi_{pj,p'j'}\rangle.\end{aligned} \tag{39}$$

The projective measurement on $|q_1^{\rm A}\rangle$ and $|q_0^{\rm A}\rangle$ is represented by the four operators $\mathcal{P}_{qq'}=|q\rangle\langle q|\otimes|q'\rangle\langle q'|\otimes I$ $(q,q'=0,1)$. The two outcomes among the possible four are of our interest, immediately after which the whole system collapses as follows:

$$\begin{aligned}|\Phi_{pj,p'j'}\rangle &\overset{|0\rangle\otimes|0\rangle\ \text{observed}}{\longmapsto} |0\rangle\ \otimes|0\rangle\otimes\frac{2s^{+}_{pj,p'j'}}{\sqrt{\mathbb{P}^{+}_{pj,p'j'}}}|\psi\rangle,\\ \text{prob. }\|2s^{+}_{pj,p'j'}|\psi\rangle\|^2 &\equiv\mathbb{P}^{+}_{pj,p'j'},\\ |\Phi_{pj,p'j'}\rangle &\overset{|1\rangle\otimes|0\rangle\ \text{observed}}{\longmapsto} |1\rangle\ \otimes|0\rangle\otimes\frac{2s^{-}_{pj,p'j'}}{\sqrt{\mathbb{P}^{-}_{pj,p'j'}}}|\psi\rangle,\\ \text{prob. }\|2s^{-}_{pj,p'j'}|\psi\rangle\|^2 &\equiv\mathbb{P}^{-}_{pj,p'j'}.\end{aligned} \tag{40, 41}$$

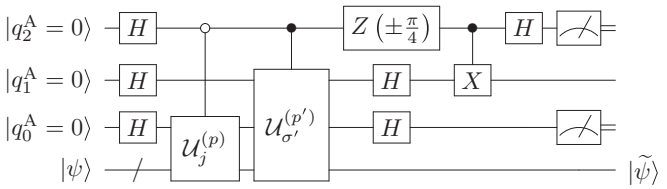

FIG. 7. Spin-charge off-diagonal circuit $\mathcal{C}^{\pm}_{pj,p'\sigma'}$ ($j = x, y$ and $\sigma' = \alpha, \beta$) for probabilistic preparation of $v^{\pm}_{pj,p'\sigma'}|\psi\rangle$ and other states from an arbitrary input state $|\psi\rangle$ and three ancillary qubits. The partial circuits defined in Figs. 3 and 5 are contained as the controlled subroutines.

3. Transition matrices via statistical sampling

We can get the transition matrices S_λ via statistical sampling similarly to the charge-charge ones. If we input $|\Psi_{\rm gs}\rangle$ to the diagonal circuit $\mathcal{C}_{pj}$ in Fig. 5 followed by a measurement and QPE for $\mathcal{H}$, the energy eigenvalue E_λ will be obtained with a probability $4S_{\lambda pj,pj}$. [See Eqs. (7) and (34).] If we use the off-diagonal circuit $\mathcal{C}_{pj,p'j'}$ in Fig. 6, on the other hand, the energy eigenvalue E_λ will be obtained with probabilities $4T^{\pm}_{\lambda pj,p'j'}$ depending on the measurement outcome. [See Eqs. (40) and (41).] The off-diagonal components of transition matrices are then calculated from Eq. (38).

E. Spin-charge responses

Having found ways to determine the charge-charge and spin-spin contributions, let us consider the determination of the spin-charge transition matrices $M_{\lambda pj,p'\sigma'}$ for $j = x, y$ and $\sigma' = \alpha, \beta$. Those involving the z component of spin, $M_{\lambda pz,p'\sigma'}$, can be calculated from the diagonal and off-diagonal components of N_λ, already obtained in Sec. II C.

1. Circuits for off-diagonal components

For combinations (p, j) and (p', σ') of spatial orbitals and spin components $j = x, y$ with $\sigma' = \alpha, \beta$, we define the two non-Hermitian auxiliary operators,

$$v^{\pm}_{pj,p'\sigma'} \equiv s_{pj} + e^{\pm i\pi/4}\frac{n_{p'\sigma'}}{2}. \tag{42}$$

Un-normalized auxiliary states $|\Psi^{\pm}_{pj,p'\sigma'}\rangle \equiv v^{\pm}_{pj,p'\sigma'}|\Psi_{\rm gs}\rangle$ can have overlaps $T^{\pm}_{\lambda pj,p'\sigma'} \equiv |\langle\Psi_\lambda|\Psi^{\pm}_{pj,p'\sigma'}\rangle|^2$ with the energy eigenstates, from which the spin-charge transition matrix elements in Eq. (8) can be calculated as

$$M_{\lambda pj,p'\sigma'} = e^{-i\pi/4}T^{+}_{\lambda pj,p'\sigma'} + e^{i\pi/4}T^{-}_{\lambda pj,p'\sigma'} - \sqrt{2}S_{\lambda pj,pj} - \frac{N_{\lambda p'\sigma',p'\sigma'}}{2\sqrt{2}}. \tag{43}$$

We construct a circuit $\mathcal{C}^{\pm}_{pj,p'\sigma'}$ equipped with three ancillary qubits by using the controlled operations of the partial circuits $\mathcal{U}_j^{(p)}$ in Fig. 5 and $\mathcal{U}_{\sigma'}^{(p')}$ in Fig. 3, as depicted in Fig. 7. The whole system consists of the ancillae and an arbitrary input register $|\psi\rangle$. Its state changes by undergoing the circuit as

$$\begin{aligned}\left|q_2^{\rm A} = 0\right\rangle \otimes \left|q_1^{\rm A} = 0\right\rangle \otimes \left|q_0^{\rm A} = 0\right\rangle \otimes |\psi\rangle \\ \longmapsto |0\rangle \otimes |0\rangle \otimes |0\rangle \otimes v^{\pm}_{pj,p'\sigma'}|\psi\rangle \\ + (|0\rangle \otimes |0\rangle \otimes |1\rangle + |1\rangle \otimes |0\rangle \otimes |1\rangle) \otimes \widetilde{s}_{pj}|\psi\rangle \\ + (|0\rangle \otimes |1\rangle \otimes |1\rangle - |1\rangle \otimes |1\rangle \otimes |1\rangle) \\ \otimes \frac{e^{\pm i\pi/4}\widetilde{n}_{p'\sigma'}}{2}|\psi\rangle \\ + |1\rangle \otimes |0\rangle \otimes |0\rangle \otimes (s_{pj} - e^{\pm i\pi/4}n_{p'\sigma'})|\psi\rangle \\ \equiv |\Phi^{\pm}_{pj,p'\sigma'}\rangle.\end{aligned} \tag{44}$$

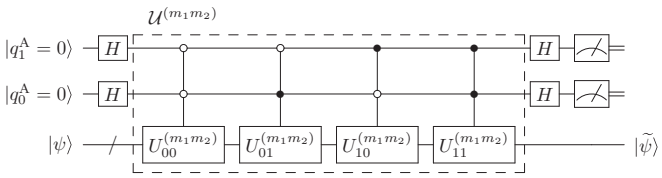

FIG. 8. Generic diagonal circuit $\mathcal{C}_{m_1m_2}$ for probabilistic preparation of $a^\dagger_{m_1}a_{m_2}|\psi\rangle$ and other states from an arbitrary input state $|\psi\rangle$ and two ancillary qubits. We define the partial circuit $\mathcal{U}^{(m_1m_2)}$ by enclosing it with dashed lines.

The projective measurement on $|q_2^{\rm A}\rangle$ and $|q_0^{\rm A}\rangle$ is represented by the four operators $\mathcal{P}_{qq'} = |q\rangle\langle q| \otimes I \otimes |q'\rangle\langle q'| \otimes I$ ($q, q' = 0, 1$). Only one of the four possible outcomes is of our interest, immediately after which the whole system collapses as follows:

$$\begin{aligned}|\Phi^{\pm}_{pj,p'\sigma'}\rangle \overset{|0\rangle\otimes|0\rangle\ \text{observed}}{\longmapsto} |0\rangle \otimes |0\rangle \otimes |0\rangle \otimes \frac{v^{\pm}_{pj,p'\sigma'}}{\sqrt{\mathbb{P}^{\pm}_{pj,p'\sigma'}}}|\psi\rangle, \\ \text{prob.}\ \|v^{\pm}_{pj,p'\sigma'}|\psi\rangle\|^2 \equiv \mathbb{P}^{\pm}_{pj,p'\sigma'}.\end{aligned} \tag{45}$$

2. Transition matrices via statistical sampling

We can get the transition matrices M_λ via statistical sampling similarly to the charge-charge and spin-spin ones. If we input $|\Psi_{\rm gs}\rangle$ to the off-diagonal circuit $\mathcal{C}^{\pm}_{pj,p'\sigma'}$ in Fig. 7 followed by a measurement and QPE for $\mathcal{H}$, the energy eigenvalue E_λ will be obtained with a probability $T^{\pm}_{\lambda pj,p'\sigma'}$. [See Eq. (45).] The off-diagonal components of transition matrices are then calculated from Eq. (43).

We provide the pseudocodes in Appendix B for the calculation procedures of response functions explained above.

F. Generic cases

Here we describe briefly the scheme for the response function involving generic one-body operators given as Eq. (12).

1. Circuits for diagonal components

For a combination of spin orbitals m_1 and m_2, we define the four unitary operators $U^{(m_1m_2)}_{\kappa\kappa'} \equiv U_{\kappa m_1}U_{\kappa' m_2}$ ($\kappa, \kappa' = 0, 1$). We construct a circuit $\mathcal{C}_{m_1m_2}$ equipped with two ancillary qubits by implementing the controlled operations for an arbitrary input register $|\psi\rangle$, as depicted in Fig. 8. It is easily confirmed that the whole state changes by undergoing the circuit as

$$\begin{aligned}\left|q_1^{\rm A} = 0\right\rangle \otimes \left|q_0^{\rm A} = 0\right\rangle \otimes |\psi\rangle \\ \longmapsto |1\rangle \otimes |0\rangle \otimes a^\dagger_{m_1}a_{m_2}|\psi\rangle + (\text{other terms}).\end{aligned} \tag{46}$$

When the target ground state is input, the projective measurement on the two ancillae leads to the probabilistic preparation

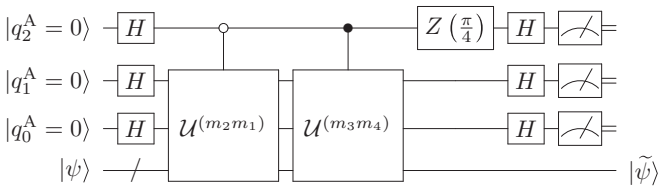

FIG. 9. Generic off-diagonal circuit $\mathcal{C}_{m_2m_1,m_3m_4}$ for probabilistic preparation of $f^{\pm}_{m_2m_1,m_3m_4}|\psi\rangle$ and other states from an arbitrary input state $|\psi\rangle$ and three ancillary qubits. The partial circuits defined in Fig. 8 are contained as the controlled subroutines.

of $a^{\dagger}_{m_1}a_{m_2}|\Psi_{\rm gs}\rangle$, for which the subsequent QPE process gives the "diagonal" matrix element $B_{\lambda m_2m_1,m_1m_2}$ [see Eq. (13)] via statistical sampling.

The charge-charge diagonal circuit $\mathcal{C}_{p\sigma}$ in Fig. 3 is a special case of the generic circuit described here.

2. *Circuits for off-diagonal components*

For mutually different combinations (m_1, m_2) and (m_3, m_4) of spin orbitals, we define the two non-Hermitian auxiliary operators,

$$f^{\pm}_{m_1m_2,m_3m_4} \equiv \frac{a^{\dagger}_{m_1}a_{m_2} \pm e^{i\pi/4}a^{\dagger}_{m_3}a_{m_4}}{2}. \tag{47}$$

Un-normalized auxiliary states $|\Psi^{\pm}_{m_1m_2,m_3m_4}\rangle \equiv f^{\pm}_{m_1m_2,m_3m_4}|\Psi_{\rm gs}\rangle$ can have overlaps $T^{\pm}_{\lambda m_1m_2,m_3m_4} \equiv |\langle\Psi_\lambda|\Psi^{\pm}_{m_1m_2,m_3m_4}\rangle|^2$ with the energy eigenstates, from which the "off-diagonal" matrix element is calculated as

$$\begin{aligned} B_{\lambda m_1m_2,m_3m_4} = {} & e^{-i\pi/4}\left(T^{+}_{\lambda m_2m_1,m_3m_4} - T^{-}_{\lambda m_2m_1,m_3m_4}\right) \\ & + e^{i\pi/4}\left(T^{+}_{\lambda m_3m_4,m_2m_1} - T^{-}_{\lambda m_3m_4,m_2m_1}\right). \end{aligned} \tag{48}$$

We construct a circuit $\mathcal{C}_{m_2m_1,m_3m_4}$ equipped with three ancillary qubits by using the controlled operations of the partial circuits defined in Fig. 8, as depicted in Fig. 9, for an arbitrary input register $|\psi\rangle$. It is easily confirmed that the whole state changes by undergoing the circuit as

$$\begin{aligned} |q_2^{\rm A} \;=\; & 0\rangle \otimes |q_1^{\rm A}=0\rangle \otimes |q_0^{\rm A}=0\rangle \otimes |\psi\rangle \\ \longmapsto\; & |0\rangle \otimes |1\rangle \otimes |0\rangle \otimes f^{+}_{m_2m_1,m_3m_4}|\psi\rangle \\ & + |1\rangle \otimes |1\rangle \otimes |0\rangle \otimes f^{-}_{m_2m_1,m_3m_4}|\psi\rangle + (\text{other terms}). \end{aligned} \tag{49}$$

When the target ground state is input, the projective measurement on the three ancillae leads to the probabilistic preparation of $|\Psi^{\pm}_{m_2m_1,m_3m_4}\rangle$. This circuit and the similarly constructed $\mathcal{C}_{m_3m_4,m_2m_1}$ allows one to calculate $B_{\lambda m_1m_2,m_3m_4}$ from Eq. (48) via statistical sampling. After obtaining the necessary matrix elements, they are put into Eq. (14) to calculate the Lehmann summation.

The charge-charge off-diagonal circuit $\mathcal{C}_{p\sigma,p'\sigma'}$ in Fig. 4 is a special case of the generic circuit described here.

III. COMPUTATIONAL DETAILS

As stated in Introduction, we simulated the measurements on qubits for obtaining the response functions of molecules by generating random numbers based on the analytically derived exact probability distributions. The computational details are described here.

We adopted STO-6G basis sets as the Cartesian Gaussian-type basis functions [30] for all the elements in our quantum chemistry calculations. The two-electron integrals between the atomic orbitals (AOs) were calculated efficiently [31]. We first performed restricted Hartree-Fock (RHF) calculations to get the orthonormalized molecular orbitals (MOs) in the target systems and calculated the two-electron integrals between them, from which we constructed the second-quantized electronic Hamiltonians.

In the FCI calculations for the large target Hilbert subspaces, we performed exact diagonalization of the electronic (not in qubit representation) Hamiltonians by using the Arnoldi method [32]. We can take the z axis as the quantization axis for spins without loss of generality since our calculations are nonrelativistic.

We calculated the FCI response functions simply by substituting the necessary quantities into Eq. (3). For the simulations of response functions from statistical sampling, we generated random numbers according to the matrix elements between the FCI energy eigenstates to mimic the measurements on ancillae and the ideal QPE procedures. We set δ in Eq. (3) to 0.01 atomic unit throughout the present study.

IV. RESULTS AND DISCUSSION

A. C_2 molecule

We used the experimental bond length of 1.242 Å [33] for a C_2 molecule in the RHF calculation and obtained the total energy $E_{\rm RHF} = -2045.2939$ eV. This system contains six electrons per spin direction which occupy the lowest six MOs, as shown in Fig. 10(a). We found via the subsequent FCI calculation with $E_{\rm FCI} = -2052.6918$ eV that the major electronic configuration in the nondegenerate many-electron

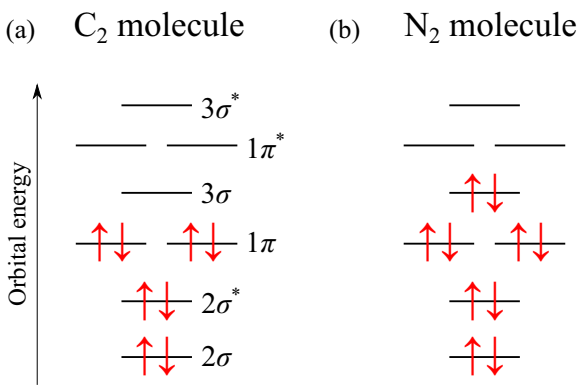

FIG. 10. Schematic illustration of RHF orbitals and their electronic occupancies for (a) a C_2 molecule and (b) an N_2 molecule. The descriptions beside the energy levels represent the orbital characters. Those with asterisks are the antibonding orbitals. The 1σ and $1\sigma^*$ MOs, coming from the $1s$ AOs of the constituent atoms, are not shown. The 1π and $1\pi^*$ MOs come mainly from the π bonding of $2p$ AOs, while the 3σ and $3\sigma^*$ MOs from the σ bonding of $2p$ AOs. The nondegenerate many-electron ground state for each system consists mainly of the same electronic configuration as the RHF one.

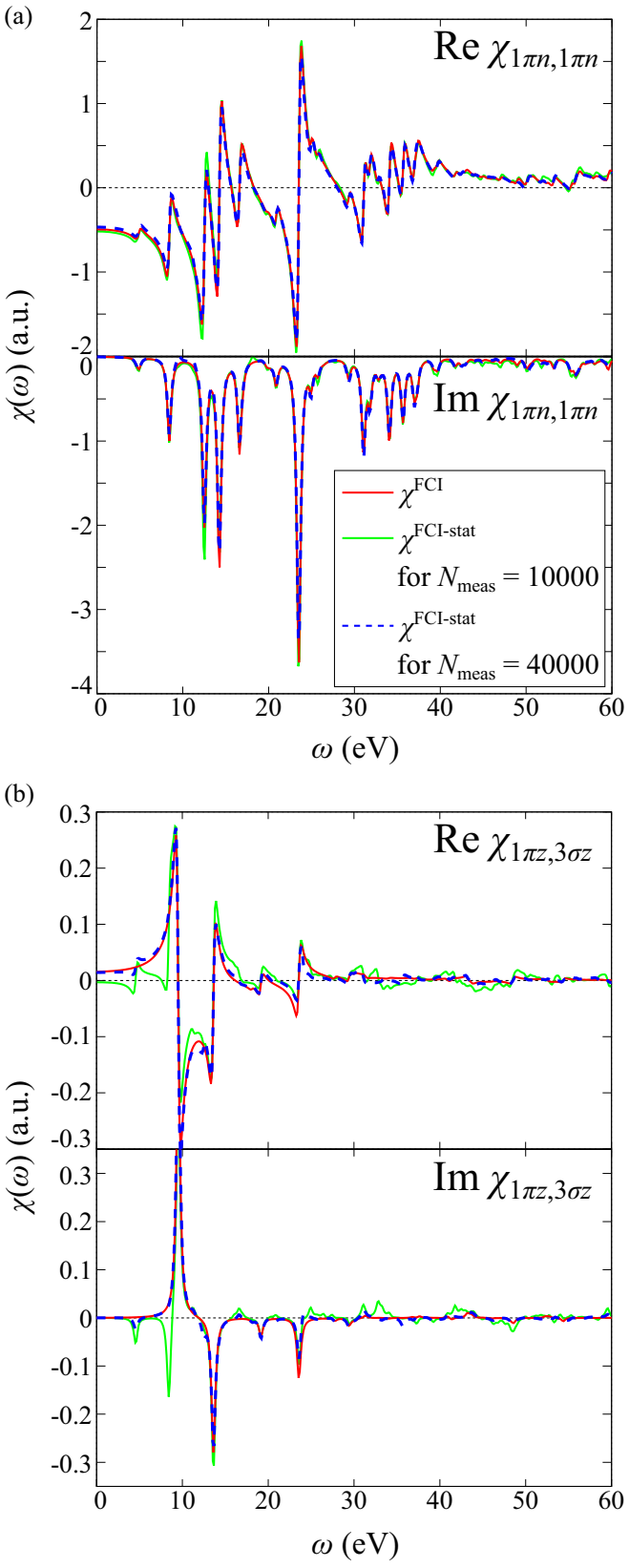

FIG. 11. The response function (a) $\chi^{\mathrm{FCI}}_{1\pi n,1\pi n}$ and (b) $\chi^{\mathrm{FCI}}_{1\pi z,3\sigma z}$ exact within the FCI solution for a C_2 molecule. The simulated ones $\chi^{\mathrm{FCI-stat}}$ for for the numbers of measurements $N_{\mathrm{meas}} = 10\,000$ and 40 000 are also shown.

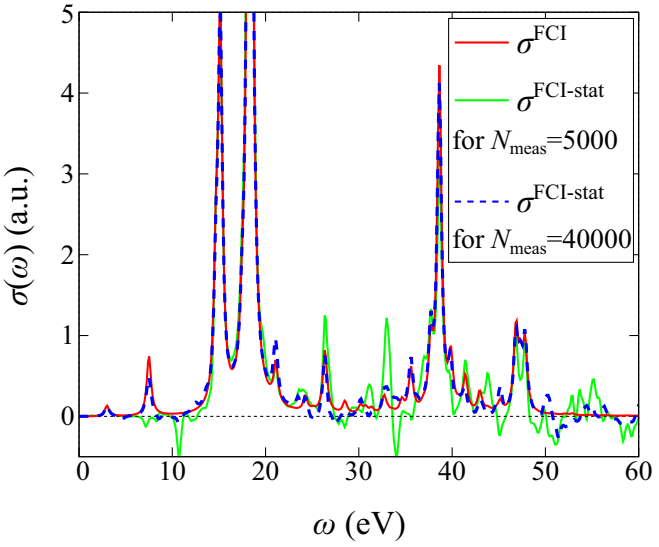

FIG. 12. The photoabsorption cross section σ^{FCI} exact within the FCI solution for a C_2 molecule. The simulated ones $\sigma^{\mathrm{FCI-stat}}$ for the numbers of measurements $N_{\mathrm{meas}} = 5000$ and 40 000 are also shown.

ground state, denoted by $X^1\Sigma_g^+$ in spectroscopic notation [34], is the same as in the RHF solution. The ground state was found via the exact diagonalization of the Hilbert subspace for $n_\alpha = n_\beta = 6$, from which we obtained the lowest 2000 among the 44 100 energy eigenvalues.

We calculated the response functions χ^{FCI} exact within the FCI solution, from which the components $\chi^{\mathrm{FCI}}_{1\pi n,1\pi n}$ and $\chi^{\mathrm{FCI}}_{1\pi z,3\sigma z}$ are plotted in Fig. 11. We also performed simulations of statistical sampling for the construction of response function $\chi^{\mathrm{FCI-stat}}$ based on our scheme and plotted those for $N_{\mathrm{meas}} = 10\,000$ and 40 000. It is seen that $\chi^{\mathrm{FCI}}_{1\pi n,1\pi n}$ in Fig. 11(a), which involves only the HOMO, is well reproduced by $\chi^{\mathrm{FCI-stat}}_{1\pi n,1\pi n}$ with $N_{\mathrm{meas}} = 10\,000$. On the other hand, $\chi^{\mathrm{FCI}}_{1\pi z,3\sigma z}$ in Fig. 11(b) is not accurately reproduced by $\chi^{\mathrm{FCI-stat}}_{1\pi n,1\pi n}$ with $N_{\mathrm{meas}} = 10\,000$. These results mean that the response involving a weak excitation channel requires a large number of measurements for its accurate reproduction, just like the situation for the GFs [19].

We calculated the photoabsorption cross section σ^{FCI} from the FCI solution, as shown in Fig. 12. By simulating the process for a generic one-body operator to obtain the matrix elements in Eq. (13), we also calculated the cross section $\sigma^{\mathrm{FCI-stat}}$ for $N_{\mathrm{meas}} = 5000$ and 40 000 and plotted it in the figure. It is seen that those from sampling can take negative values despite the original definition in Eq. (15), which is ensured to be non-negative. It is due to our naïve implementation of Eq. (48) by using random numbers without considering any symmetry. The major peaks in σ^{FCI} were well reproduced by $\sigma^{\mathrm{FCI-stat}}$ with the smaller N_{meas}, while the detailed structure between them required the larger N_{meas} for the accurate reproduction. Since symmetry-adapted construction of transition matrix elements should reduce the necessary total number of measurements and physically appropriate results, such techniques will be useful as well as in VQE calculations [35].

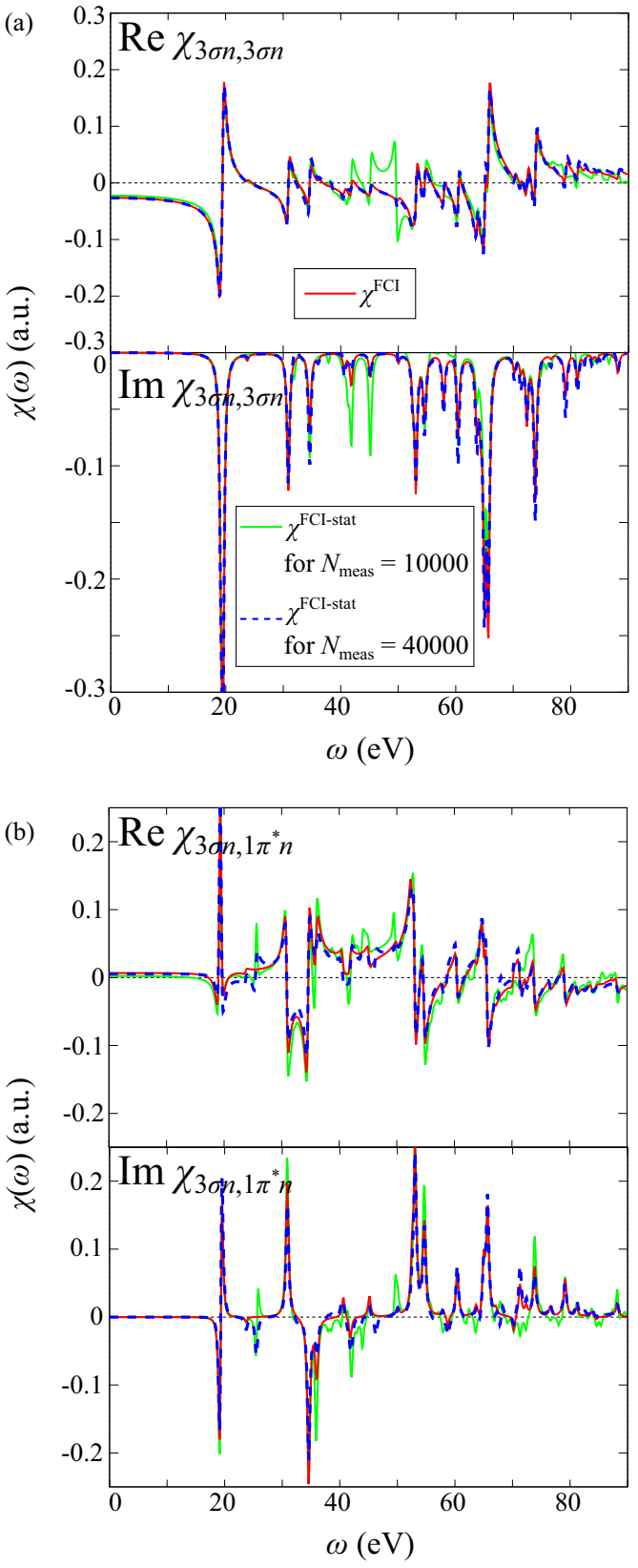

FIG. 13. The response function (a) $\chi^{\mathrm{FCI}}_{3\sigma n,3\sigma n}$ and (b) $\chi^{\mathrm{FCI}}_{3\sigma n,1\pi^* n}$ exact within the FCI solution for an N_2 molecule. The simulated ones $\chi^{\mathrm{FCI-stat}}$ for the numbers of measurements $N_{\mathrm{meas}} = 10\,000$ and 40 000 are also shown.

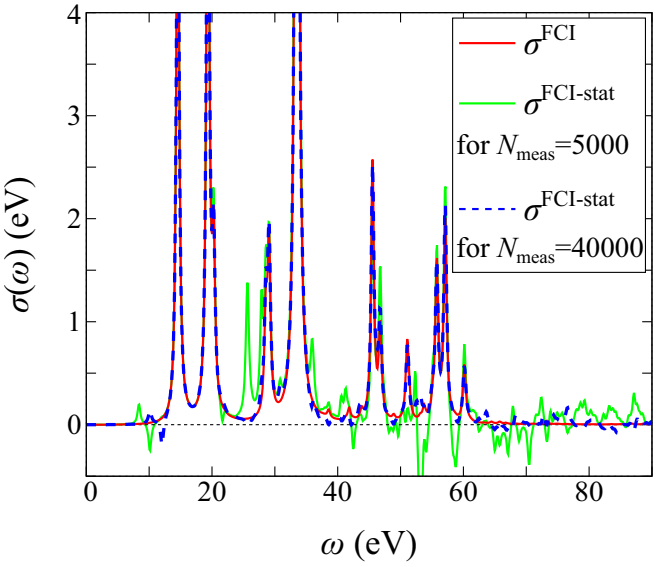

FIG. 14. The photoabsorption cross section σ^{FCI} exact within the FCI solution for an N_2 molecule. The simulated ones $\sigma^{\mathrm{FCI-stat}}$ for the numbers of measurements $N_{\mathrm{meas}} = 5000$ and 40 000 are also shown.

In a more practical setup where the QPE procedure is not ideal, the resolution and the reliability of two-qubit gates in the QPE procedure will have significant impacts on the results. The adequate number of measurements should thus be discussed by considering specific setups.

B. N_2 molecule

We used the experimental bond length of 1.098 Å [36] for an N_2 molecule in the RHF calculation and obtained the total energy $E_{\mathrm{RHF}} = -2953.5952$ eV. This system contains seven electrons per spin direction which occupy the lowest seven MOs, as shown in Fig. 10(b). We found via the subsequent FCI calculation with $E_{\mathrm{FCI}} = -2957.9124$ eV that the major electronic configuration in the nondegenerate many-electron ground state is $X^1\Sigma_g^+$ [34], the same as in the RHF solution. The ground state was found via the exact diagonalization of the Hilbert subspace for $n_\alpha = n_\beta = 7$, from which we obtained the lowest 2000 among the 14 400 energy eigenvalues.

We calculated the response functions from the FCI solution, from which the components $\chi^{\mathrm{FCI}}_{3\sigma n,3\sigma n}$ and $\chi^{\mathrm{FCI}}_{3\sigma n,1\pi^* n}$ are plotted in Fig. 13. We also performed simulations for the construction of $\chi^{\mathrm{FCI-stat}}$ and plotted those for $N_{\mathrm{meas}} = 10\,000$ and 40 000. It is seen that $\chi^{\mathrm{FCI}}_{3\sigma n,3\sigma n}$ in Fig. 13(a), which involves only the HOMO, is not well reproduced by $\chi^{\mathrm{FCI-stat}}_{3\sigma n,3\sigma n}$ with $N_{\mathrm{meas}} = 10\,000$, in contrast to the C_2 molecule case. Since the strength of $\chi^{\mathrm{FCI}}_{3\sigma n,1\pi^* n}$ in Fig. 13(b) is similar to that of $\chi^{\mathrm{FCI}}_{3\sigma n,3\sigma n}$, $N_{\mathrm{meas}} = 10\,000$ is not sufficient for the accurate reproduction of correct values as well. We found that $\chi^{\mathrm{FCI}}_{3\sigma z,1\pi^* z}$ (not shown) is much weaker and even $N_{\mathrm{meas}} = 40\,000$ is insufficient for obtaining good $\chi^{\mathrm{FCI-stat}}_{3\sigma z,1\pi^* z}$.

We calculated the photoabsorption cross section σ^{FCI} from the FCI solution, as shown in Fig. 14. Those from simulations of measurements $\sigma^{\mathrm{FCI-stat}}$ for $N_{\mathrm{meas}} = 5000$ and 40 000 are also shown in the figure.

V. CONCLUSIONS

We proposed a scheme for the construction of linear-response functions of an interacting electronic system via QPE and statistical sampling on a quantum computer. By using the unitary decomposition of electronic operators for avoiding the difficulty due to their nonunitarity, we provided the circuits equipped with at most three ancillae for probabilistic preparation of qubit states on which the necessary nonunitary operators have acted. We performed simulations of such construction of the response functions for C_2 and N_2 molecules by comparing with the accurate ones based on the FCI calculations. It was found that the accurate detection of subtle structures coming from the weak poles in the response functions requires a large number of measurements.

Since the unitary decomposition of electronic operators is applicable regardless of the adopted qubit representation, an electronic state on which an arbitrary product of the creation and annihilation operators has acted can be prepared at least probabilistically. The quality of results for our approach comes mainly along with that of QPE procedure, implying that the feasibility of our approach may be promising for small systems which have been already treated on realized quantum computers such as an H_2 molecule. The approach described in this study enables one to access not only the response functions and GFs but also various physical quantities on a quantum computer. Invention and enrichment of tools for such properties will enhance the practical use of quantum computers for material simulations.

ACKNOWLEDGMENTS

This research was supported by MEXT as Exploratory Challenge on Post-K computer (Frontiers of Basic Science: Challenging the Limits) and Grants-in-Aid for Scientific Research (A) (Grant No. 18H03770) from Japan Society for the Promotion of Science (JSPS).

APPENDIX A: PROOF FOR A GENERIC PROBABILISTIC STATE PREPARATION

1. Proof

Here we provide the proof for the validity of circuit $\mathcal{C}_{\mathcal{O}}$ in Fig. 1 for probabilistic state preparation. $\mathcal{C}_{\mathcal{O}}$ is characterized by the 2^n-1 parameters, $\theta^{(n)}, \theta_0^{(n-1)}, \theta_1^{(n-1)}, \theta_{00}^{(n-2)}, \theta_{01}^{(n-2)}, \theta_{10}^{(n-2)}, \theta_{11}^{(n-2)}, \ldots, \theta_{1\cdots1}^{(1)}$. For an arbitrary input state $|\psi\rangle$ and the linear combination $\mathcal{O}$ of unitaries in Eq. (1), $\mathcal{O}|\psi\rangle$ up to a normalization constant can be prepared by setting the parameters to appropriate values, as demonstrated below. We can assume that the coefficients in Eq. (1) are positive real values without loss of generality since each of the phase factors can be absorbed into the unitary coupled to it.

We use the notation $|\Phi_n\rangle \equiv |0\rangle^{\otimes n} \otimes |\psi\rangle$, $H_n \equiv H^{\otimes n} \otimes I$, and $R_y(-2\theta)|q\rangle \equiv |q,\theta\rangle$ for $q=0,1$. The action of circuit on the initial state $|\Phi_n\rangle$ can be tracked by referring to the recursive definition in Fig. 2. Specifically, we find

$$\begin{aligned}
\mathcal{C}^{(n)}H_n|\Phi_n\rangle &= \frac{|0,\theta^{(n)}\rangle}{\sqrt{2}} \otimes \mathcal{C}_0^{(n-1)}H_{n-1}|\Phi_{n-1}\rangle + \frac{|1,\theta^{(n)}\rangle}{\sqrt{2}} \otimes \mathcal{C}_1^{(n-1)}H_{n-1}|\Phi_{n-1}\rangle \\
&= \frac{|0,\theta^{(n)}\rangle}{\sqrt{2}} \otimes \left[\frac{|0,\theta_0^{(n-1)}\rangle}{\sqrt{2}} \otimes \mathcal{C}_{00}^{(n-2)}H_{n-2}|\Phi_{n-2}\rangle + \frac{|1,\theta_0^{(n-1)}\rangle}{\sqrt{2}} \otimes \mathcal{C}_{01}^{(n-2)}H_{n-2}|\Phi_{n-2}\rangle \right] \\
&\quad + \frac{|1,\theta^{(n)}\rangle}{\sqrt{2}} \otimes \left[\frac{|0,\theta_1^{(n-1)}\rangle}{\sqrt{2}} \otimes \mathcal{C}_{10}^{(n-2)}H_{n-2}|\Phi_{n-2}\rangle + \frac{|1,\theta_1^{(n-1)}\rangle}{\sqrt{2}} \otimes \mathcal{C}_{11}^{(n-2)}H_{n-2}|\Phi_{n-2}\rangle \right] = \cdots \\
&= \frac{1}{2^{n/2}}|0,\theta^{(n)}\rangle \otimes |0,\theta_0^{(n-1)}\rangle \otimes |0,\theta_{00}^{(n-2)}\rangle \otimes \cdots \otimes |0,\theta_{0\cdots0}^{(1)}\rangle \otimes U_{0\cdots0}|\psi\rangle + \cdots \\
&\quad + \frac{1}{2^{n/2}}|1,\theta^{(n)}\rangle \otimes |1,\theta_1^{(n-1)}\rangle \otimes |1,\theta_{11}^{(n-2)}\rangle \otimes \cdots \otimes |1,\theta_{1\cdots1}^{(1)}\rangle \otimes U_{1\cdots1}|\psi\rangle. \qquad \text{(A1)}
\end{aligned}$$

For each bit string k of length n, U_k appears only once on the right-hand side of Eq. (A1). If the outcome of a projective measurement on the n ancillae is $|0\rangle^{\otimes n}$, the whole state collapses immediately after the measurement as follows:

$$\begin{aligned}
\mathcal{C}^{(n)}H_n|\Phi_n\rangle \overset{|0\rangle^{\otimes n}\text{ observed}}{\longmapsto}\ & |0\rangle^{\otimes n} \otimes \frac{1}{2^{n/2}} \\
& \times \Big[\cos\theta^{(n)} \cos\theta_0^{(n-1)} \cos\theta_{00}^{(n-2)} \cdots \cos\theta_{0\cdots0}^{(2)} \cos\theta_{0\cdots00}^{(1)} U_{0\cdots000} \\
& + \cos\theta^{(n)} \cos\theta_0^{(n-1)} \cos\theta_{00}^{(n-2)} \cdots \cos\theta_{0\cdots0}^{(2)} \sin\theta_{0\cdots00}^{(1)} U_{0\cdots001} \\
& \vdots \\
& + \sin\theta^{(n)} \sin\theta_1^{(n-1)} \sin\theta_{11}^{(n-2)} \cdots \sin\theta_{1\cdots1}^{(2)} \cos\theta_{1\cdots11}^{(1)} U_{1\cdots110} \\
& + \sin\theta^{(n)} \sin\theta_1^{(n-1)} \sin\theta_{11}^{(n-2)} \cdots \sin\theta_{1\cdots1}^{(2)} \sin\theta_{1\cdots11}^{(1)} U_{1\cdots111} \Big] |\psi\rangle. \qquad \text{(A2)}
\end{aligned}$$

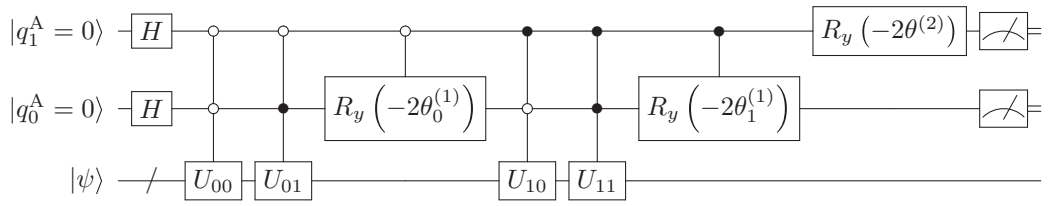

FIG. 15. Circuit $\mathcal{C}_{\mathcal{O}}$ for $n=2$ as a special case of that in Fig. 1.

We derived the expression above by using $|0,\theta\rangle = \cos\theta|0\rangle - \sin\theta|1\rangle$ and $|1,\theta\rangle = \sin\theta|0\rangle + \cos\theta|1\rangle$.

In order for the resultant state to be proportional to $\mathcal{O}|\psi\rangle$, we first determine the 2^{n-1} parameters $\theta^{(1)}_{0\cdots00},\ldots,\theta^{(1)}_{1\cdots11}$ (each having a bit string of length $n-1$) such that

$$\tan\theta^{(1)}_{0\cdots00} = \frac{c_{0\cdots001}}{c_{0\cdots000}},\ \tan\theta^{(1)}_{0\cdots01} = \frac{c_{0\cdots011}}{c_{0\cdots010}},\ldots,\tan\theta^{(1)}_{1\cdots11} = \frac{c_{1\cdots111}}{c_{1\cdots110}}. \tag{A3}$$

Next we determine the 2^{n-2} parameters $\theta^{(2)}_{0\cdots00},\ldots,\theta^{(2)}_{1\cdots11}$ (each having a bit string of length $n-2$) such that

$$\frac{\cos\theta^{(1)}_{0\cdots001}}{\cos\theta^{(1)}_{0\cdots000}}\tan\theta^{(2)}_{0\cdots00} = \frac{c_{0\cdots0010}}{c_{0\cdots0000}},\ \frac{\cos\theta^{(1)}_{0\cdots011}}{\cos\theta^{(1)}_{0\cdots010}}\tan\theta^{(2)}_{0\cdots01} = \frac{c_{0\cdots0110}}{c_{0\cdots0100}},\ldots,\frac{\cos\theta^{(1)}_{1\cdots111}}{\cos\theta^{(1)}_{1\cdots110}}\tan\theta^{(2)}_{1\cdots11} = \frac{c_{1\cdots1110}}{c_{1\cdots1100}}. \tag{A4}$$

All the remaining parameters can also be determined in this way, so that the circuit $\mathcal{C}_{\mathcal{O}}$ allows one to prepare the desired state $\mathcal{O}|\psi\rangle$ probabilistically. It is noted that the probability $\langle\psi|\mathcal{O}^\dagger\mathcal{O}|\psi\rangle$ is determined not by the artifact (the number n of ancillae the user has introduced), but by the physics (the quantum state $\mathcal{O}|\psi\rangle$ itself) regardless of n. This fact also means that the probability of "success" in the state preparation gives the information about the normalization constant, which can be as important as the desired state. In this sense, measurement results other than $|0\rangle^{\otimes n}$ are neither failures nor waste of time.

The construction procedure described above should be understood as a starting point for a generic nonunitary operator. There can be room for making the circuit more efficient by considering the characteristics of the operator and/or the states you want. For example, the circuit in Fig. 3 does not contain a rotation gate and only one of the two ancillae needs to be measured. It works thanks to the Fermi statistics. Another interesting point is seen in the circuit in Fig. 4, which can prepare the two important states $n^+_{p\sigma,p'\sigma'}|\psi\rangle$ and $n^-_{p\sigma,p'\sigma'}|\psi\rangle$. [See Eqs. (27) and (28).]

2. Example for $n=2$

An example for the determination of parameters for $\mathcal{C}_{\mathcal{O}}$ with $n=2$ is provided here. The circuit is parametrized by $\theta^{(1)}_0$, $\theta^{(1)}_1$, and $\theta^{(2)}$, as depicted in Fig. 15. The whole state immediately before a measurement is

$$\begin{aligned}\mathcal{C}^{(2)}H_2|\Phi_2\rangle = |0\rangle^{\otimes2}\otimes\tfrac{1}{2}\big[&\cos\theta^{(2)}\cos\theta^{(1)}_0U_{00} + \cos\theta^{(2)}\sin\theta^{(1)}_0U_{01} + \sin\theta^{(2)}\cos\theta^{(1)}_1U_{10} + \sin\theta^{(2)}\sin\theta^{(1)}_1U_{11}\big]|\psi\rangle\\ &+ (\text{terms involving other ancillary states}).\end{aligned} \tag{A5}$$

The probabilistic state preparation is possible by setting the three parameters in the manner described above. $\theta^{(1)}_0$ and $\theta^{(1)}_1$ are determined by the conditions,

$$\tan\theta^{(1)}_0 = \frac{c_{01}}{c_{00}},\ \tan\theta^{(1)}_1 = \frac{c_{11}}{c_{10}}, \tag{A6}$$

from which $\theta^{(2)}$ is determined by the condition,

$$\frac{\cos\theta^{(1)}_1}{\cos\theta^{(1)}_0}\tan\theta^{(2)} = \frac{c_{10}}{c_{00}}. \tag{A7}$$

APPENDIX B: PSEUDOCODES

Here we provide the pseudocodes for the calculation of response functions proposed in the present study. We assume that all the energy eigenvalues of N-electron states have been obtained before entering the main procedure given just below.

1. Main procedure

Here is the main procedure. It calls directly or indirectly all the other procedures provided in this Appendix.

Procedure 1 Calculation of charge and spin response functions via statistical sampling.

Input:
Hamiltonian $\mathcal{H}$, number of spatial orbitals n_{orbs}, N-electron ground state $|\Psi_{\mathrm{gs}}\rangle$ with its energy E^N_{gs}, energy eigenvalues E^N_λ, real frequency ω, small positive constant δ, number of measurements N_{meas} for each component
Output:
Response functions $\chi(\omega)$

function CALCRESPFUNCS ($\mathcal{H}$, n_{orbs}, $|\Psi_{\mathrm{gs}}\rangle$, E^N_{gs}, E^N, ω, δ, N_{meas})
  for λ
    $d_{\lambda\pm} := \pm(\omega + i\delta) - (E^N_\lambda - E^N_{\mathrm{gs}})$
  $\chi^{\mathrm{tmp}} := 0$
  for $p = 1, \ldots, n_{\mathrm{orbs}}$ ▷ Diagonal components
    for $\sigma = \alpha, \beta$ ▷ Charge-charge contributions
      $N_{p\sigma,p\sigma} :=$ AMPLSCHARGEDIAG ($\mathcal{H}$, $|\Psi_{\mathrm{gs}}\rangle$, E^N, p, σ, N_{meas})
      for λ
        $\chi^{\mathrm{tmp}}_{p\sigma,p\sigma} += N_{\lambda p\sigma,p\sigma}/d_{\lambda+} + N_{\lambda p\sigma,p\sigma}/d_{\lambda-}$
    for $j = x, y$ ▷ Spin-spin contributions
      $S_{pj,pj} :=$ AMPLSSPINDIAG ($\mathcal{H}$, $|\Psi_{\mathrm{gs}}\rangle$, E^N, p, j, N_{meas})
      for λ
        $\chi^{\mathrm{tmp}}_{pj,pj} += S_{\lambda pj,pj}/d_{\lambda+} + S_{\lambda pj,pj}/d_{\lambda-}$
  for $p, p' = 1, \ldots, n_{\mathrm{orbs}}$ $(p \geqq p')$ ▷ Off-Diagonal components
    for $\sigma, \sigma' = \alpha, \beta$ ▷ Charge-charge contributions
      if $p > p'$ **or** $(p == p'$ **and** $\sigma == \beta$ **and** $\sigma' == \alpha)$ **then**
        $N_{p\sigma,p'\sigma'} :=$ AMPLSCHARGEOFFDIAG ($\mathcal{H}$, $|\Psi_{\mathrm{gs}}\rangle$, E^N, p, p', σ, σ', N_{meas})
        for λ
          $\chi^{\mathrm{tmp}}_{p\sigma,p'\sigma'} += N_{\lambda p\sigma,p'\sigma'}/d_{\lambda+} + N^*_{\lambda p\sigma,p'\sigma'}/d_{\lambda-}$, $\chi^{\mathrm{tmp}}_{p'\sigma',p\sigma} += N^*_{\lambda p\sigma,p'\sigma'}/d_{\lambda+} + N_{\lambda p\sigma,p'\sigma'}/d_{\lambda-}$
    for $j, j' = x, y$ ▷ Spin-spin contributions
      if $p > p'$ **or** $(p == p'$ **and** $j == y$ **and** $j' == x)$ **then**
        $S_{pj,p'j'} :=$ AMPLSSPINOFFDIAG ($\mathcal{H}$, $|\Psi_{\mathrm{gs}}\rangle$, E^N, p, p', j, j', N_{meas})
        for λ
          $\chi^{\mathrm{tmp}}_{pj,p'j'} += S_{\lambda pj,p'j'}/d_{\lambda+} + S^*_{\lambda pj,p'j'}/d_{\lambda-}$, $\chi^{\mathrm{tmp}}_{p'j',pj} += S^*_{\lambda pj,p'j'}/d_{\lambda+} + S_{\lambda pj,p'j'}/d_{\lambda-}$
    for $j = x, y, \sigma' = \alpha, \beta$ ▷ Spin-charge contributions
      $M_{pj,p'\sigma'} :=$ AMPLSSPINCHARGEOFFDIAG ($\mathcal{H}$, $|\Psi_{\mathrm{gs}}\rangle$, E^N, p, p', j, σ', $S_{pj,pj}$, $N_{p'\sigma',p'\sigma'}$, N_{meas})
      for λ
        $\chi^{\mathrm{tmp}}_{pj,p'\sigma'} += M_{\lambda pj,p'\sigma'}/d_{\lambda+} + M^*_{\lambda pj,p'\sigma'}/d_{\lambda-}$, $\chi^{\mathrm{tmp}}_{p'\sigma',pj} += M^*_{\lambda pj,p'\sigma'}/d_{\lambda+} + M_{\lambda pj,p'\sigma'}/d_{\lambda-}$
  for $p, p' = 1, \ldots, n_{\mathrm{orbs}}$ ▷ Representation for (n, x, y, z) from (α, β, x, y)
    $\chi_{pn,p'n} := \chi^{\mathrm{tmp}}_{p\alpha,p'\alpha} + \chi^{\mathrm{tmp}}_{p\alpha,p'\beta} + \chi^{\mathrm{tmp}}_{p\beta,p'\alpha} + \chi^{\mathrm{tmp}}_{p\beta,p'\beta}$, $\chi_{pn,p'z} := \left(\chi^{\mathrm{tmp}}_{p\alpha,p'\alpha} - \chi^{\mathrm{tmp}}_{p\alpha,p'\beta} + \chi^{\mathrm{tmp}}_{p\beta,p'\alpha} - \chi^{\mathrm{tmp}}_{p\beta,p'\beta}\right)/2$
    $\chi_{pz,p'n} := \left(\chi^{\mathrm{tmp}}_{p\alpha,p'\alpha} + \chi^{\mathrm{tmp}}_{p\alpha,p'\beta} - \chi^{\mathrm{tmp}}_{p\beta,p'\alpha} - \chi^{\mathrm{tmp}}_{p\beta,p'\beta}\right)/2$, $\chi_{pz,p'z} := \left(\chi^{\mathrm{tmp}}_{p\alpha,p'\alpha} - \chi^{\mathrm{tmp}}_{p\alpha,p'\beta} - \chi^{\mathrm{tmp}}_{p\beta,p'\alpha} + \chi^{\mathrm{tmp}}_{p\beta,p'\beta}\right)/4$
    for $j = x, y$
      $\chi_{pn,p'j} := \chi^{\mathrm{tmp}}_{p\alpha,p'j} + \chi^{\mathrm{tmp}}_{p\beta,p'j}$, $\chi_{pz,p'j} := \left(\chi^{\mathrm{tmp}}_{p\alpha,p'j} - \chi^{\mathrm{tmp}}_{p\beta,p'j}\right)/2$
      $\chi_{pj,p'n} := \chi^{\mathrm{tmp}}_{pj,p'\alpha} + \chi^{\mathrm{tmp}}_{pj,p'\beta}$, $\chi_{pj,p'z} := \left(\chi^{\mathrm{tmp}}_{pj,p'\alpha} - \chi^{\mathrm{tmp}}_{pj,p'\beta}\right)/2$
    for $j, j' = x, y$
      $\chi_{pj,p'j'} := \chi^{\mathrm{tmp}}_{pj,p'j'}$
  return χ

2. Charge-charge contributions

The following procedures calculate the matrix elements in the manner described in Sec. II C.

a. Diagonal components

Procedure 2 Calculation of diagonal components of transition matrices.

function AMPLSCHARGEDIAG ($\mathcal{H}$, $|\Psi_{\rm gs}\rangle$, E^N, p, σ, $N_{\rm meas}$)
  $N_{p\sigma,p\sigma} := 0$
  for $m = 1, \ldots, N_{\rm meas}$
    Input $|\Psi_{\rm gs}\rangle$ to $\mathcal{C}_{p\sigma}$ and measure the ancilla $|q_0^{\rm A}\rangle$ ▷ Circuit in Fig. 3
    if $|q_0^{\rm A}\rangle == |0\rangle$ **then**
      $E :=$ QPE($|\widetilde{\Psi}\rangle$, $\mathcal{H}$), Find E among $\{E_\lambda^N\}_\lambda$ ▷ For the register $|\widetilde{\Psi}\rangle$ coming out of the circuit
      $N_{\lambda p\sigma,p\sigma} += 1$
  $N_{p\sigma,p\sigma} *= 1/N_{\rm meas}$
  return $N_{p\sigma,p\sigma}$

b. Off-diagonal components

Procedure 3 Calculation of off-diagonal components of transition matrices.

function AMPLSCHARGEOFFDIAG ($\mathcal{H}$, $|\Psi_{\rm gs}\rangle$, E^N, p, p', σ, σ', $N_{\rm meas}$)
  $T^{\pm}_{p\sigma,p'\sigma'} :=$ AMPLSCHARGEAUX ($\mathcal{H}$, $|\Psi_{\rm gs}\rangle$, E^N, p, p', σ, σ', $N_{\rm meas}$)
  $T^{\pm}_{p'\sigma',p\sigma} :=$ AMPLSCHARGEAUX ($\mathcal{H}$, $|\Psi_{\rm gs}\rangle$, E^N, p', p, σ', σ, $N_{\rm meas}$)
  for λ
    $N_{\lambda p\sigma,p'\sigma'} := e^{-i\pi/4}(T^{+}_{\lambda p\sigma,p'\sigma'} - T^{-}_{\lambda p\sigma,p'\sigma'}) + e^{i\pi/4}(T^{+}_{\lambda p'\sigma',p\sigma} - T^{-}_{\lambda p'\sigma',p\sigma})$ ▷ See eq. (25)
  return $N_{p\sigma,p'\sigma'}$

Procedure 4 Calculation of transition amplitudes for auxiliary states.

function AMPLSCHARGEAUX ($\mathcal{H}$, $|\Psi_{\rm gs}^N\rangle$, E^N, p, p', σ, σ', $N_{\rm meas}$)
  $T^{\pm}_{p\sigma,p'\sigma'} := 0$
  for $m = 1, \ldots, N_{\rm meas}$
    Input $|\Psi_{\rm gs}\rangle$ to $\mathcal{C}_{p\sigma,p'\sigma'}$ and measure the ancillae $|q_2^{\rm A}\rangle$ and $|q_1^{\rm A}\rangle$ ▷ Circuit in Fig. 4
    if $|q_2^{\rm A}\rangle \otimes |q_1^{\rm A}\rangle == |0\rangle \otimes |1\rangle$ **then**
      $E :=$ QPE($|\widetilde{\Psi}\rangle$, $\mathcal{H}$), Find E among $\{E_\lambda^N\}_\lambda$ ▷ For the register $|\widetilde{\Psi}\rangle$ coming out of the circuit
      $T^{+}_{\lambda p\sigma,p'\sigma'} += 1$
    else if $|q_2^{\rm A}\rangle \otimes |q_1^{\rm A}\rangle == |1\rangle \otimes |1\rangle$ **then**
      $E :=$ QPE($|\widetilde{\Psi}\rangle$, $\mathcal{H}$), Find E among $\{E_\lambda^N\}_\lambda$ ▷ For the register $|\widetilde{\Psi}\rangle$ coming out of the circuit
      $T^{-}_{\lambda p\sigma,p'\sigma'} += 1$
  $T^{\pm}_{p\sigma,p'\sigma'} *= 1/N_{\rm meas}$
  return $T^{\pm}_{p\sigma,p'\sigma'}$

3. Spin-spin contributions

The following procedures calculate the matrix elements in the manner described in Sec. II D.

a. Diagonal components

Procedure 5 Calculation of diagonal components of transition matrices.

function AMPLSSPINDIAG ($\mathcal{H}$, $|\Psi_{\rm gs}\rangle$, E^N, p, j, $N_{\rm meas}$)
  $S_{pj,pj} := 0$
  for $m = 1, \ldots, N_{\rm meas}$
    Input $|\Psi_{\rm gs}\rangle$ to $\mathcal{C}_{pj}$ and measure the ancilla $|q^{\rm A}\rangle$ ▷ Circuit in Fig. 5
    if $|q^{\rm A}\rangle == |0\rangle$ **then**
      $E :=$ QPE($|\widetilde{\Psi}\rangle$, $\mathcal{H}$), Find E among $\{E^N_\lambda\}_\lambda$ ▷ For the register $|\widetilde{\Psi}\rangle$ coming out of the circuit
      $S_{\lambda pj,pj} += 1$
  $S_{pj,pj} *= 1/(4N_{\rm meas})$
  return $S_{pj,pj}$

b. Off-diagonal components

Procedure 6 Calculation of off-diagonal components of transition matrices.

function AMPLSSPINOFFDIAG ($\mathcal{H}$, $|\Psi_{\rm gs}\rangle$, E^N, p, p', j, j', $N_{\rm meas}$)
  $T^{\pm}_{pj,p'j'} :=$ AMPLSSPINAUX ($\mathcal{H}$, $|\Psi_{\rm gs}\rangle$, E^N, p, p', j, j', $N_{\rm meas}$)
  $T^{\pm}_{p'j',pj} :=$ AMPLSSPINAUX ($\mathcal{H}$, $|\Psi_{\rm gs}\rangle$, E^N, p', p, j', j, $N_{\rm meas}$)
  for λ
    $S_{\lambda pj,p'j'} := e^{-i\pi/4}(T^{+}_{\lambda pj,p'j'} - T^{-}_{\lambda pj,p'j'}) + e^{i\pi/4}(T^{+}_{\lambda p'j',pj} - T^{-}_{\lambda p'j',pj})$ ▷ See eq. (38)
  return $S_{pj,p'j'}$

Procedure 7 Calculation of transition amplitudes for auxiliary states.

function AMPLSSPINAUX ($\mathcal{H}$, $|\Psi_{\rm gs}\rangle$, E^N, p, p', j, j', $N_{\rm meas}$)
  $T^{\pm}_{pj,p'j'} := 0$
  for $m = 1, \ldots, N_{\rm meas}$
    Input $|\Psi_{\rm gs}\rangle$ to $\mathcal{C}_{pj,p'j'}$ and measure the ancillae $|q^{\rm A}_1\rangle$ and $|q^{\rm A}_0\rangle$ ▷ Circuit in Fig. 6
    if $|q^{\rm A}_1\rangle \otimes |q^{\rm A}_0\rangle == |0\rangle \otimes |0\rangle$ **then**
      $E :=$ QPE($|\widetilde{\Psi}\rangle$, $\mathcal{H}$), Find E among $\{E^N_\lambda\}_\lambda$ ▷ For the register $|\widetilde{\Psi}\rangle$ coming out of the circuit
      $T^{+}_{\lambda pj,p'j'} += 1$
    else if $|q^{\rm A}_1\rangle \otimes |q^{\rm A}_0\rangle == |1\rangle \otimes |0\rangle$ **then**
      $E :=$ QPE($|\widetilde{\Psi}\rangle$, $\mathcal{H}$), Find E among $\{E^N_\lambda\}_\lambda$ ▷ For the register $|\widetilde{\Psi}\rangle$ coming out of the circuit
      $T^{-}_{\lambda pj,p'j'} += 1$
  $T^{\pm}_{pj,p'j'} *= 1/(4N_{\rm meas})$
  return $T^{\pm}_{pj,p'j'}$

4. Spin-charge contributions

The following procedures calculate the matrix elements in the manner described in Sec. II E.

Procedure 8 Calculation of off-diagonal components of transition matrices.

function AMPLSSPINCHARGEOFFDIAG ($\mathcal{H}$, $|\Psi_{\rm gs}\rangle$, E^N, p, p', j, σ', $S_{pj,pj}$, $N_{p'\sigma',p'\sigma'}$, $N_{\rm meas}$)
  $T^{\pm}_{pj,p'\sigma'} :=$ AMPLSSPINCHARGEAUX ($\mathcal{H}$, $|\Psi_{\rm gs}\rangle$, E^N, $\pm$, p, p', j, σ', $N_{\rm meas}$)
  for λ
    $M_{\lambda pj,p'\sigma'} := e^{-i\pi/4}T^{+}_{\lambda pj,p'\sigma'} + e^{i\pi/4}T^{-}_{\lambda pj,p'\sigma'} - \sqrt{2}S_{\lambda pj,pj} - \frac{N_{\lambda p'\sigma',p'\sigma'}}{2\sqrt{2}}$ ▷ See eq. (43)
  return $M_{pj,p'\sigma'}$

Procedure 9 Calculation of transition amplitudes for auxiliary states.

function AMPLSSPINCHARGEAUX ($\mathcal{H}$, $|\Psi_{\rm gs}\rangle$, E^N, v, p, p', j, σ', $N_{\rm meas}$)
  $T^v_{pj,p'\sigma'} := 0$
  for $m = 1, \ldots, N_{\rm meas}$
    Input $|\Psi_{\rm gs}\rangle$ to $\mathcal{C}^v_{pj,p'\sigma'}$ and measure the ancillae $|q_2^{\rm A}\rangle$ and $|q_0^{\rm A}\rangle$ ▷ Circuit in Fig. 7
    if $|q_2^{\rm A}\rangle \otimes |q_0^{\rm A}\rangle == |0\rangle \otimes |0\rangle$ **then**
      $E :=$ QPE($|\widetilde{\Psi}\rangle$, $\mathcal{H}$), Find E among $\{E^N_\lambda\}_\lambda$ ▷ For the register $|\widetilde{\Psi}\rangle$ coming out of the circuit
      $T^v_{\lambda pj,p'\sigma'} += 1$
  $T^v_{pj,p'\sigma'} *= 1/N_{\rm meas}$
  return $T^v_{pj,p'\sigma'}$

[1] M. A. Nielsen and I. L. Chuang, *Quantum Computation and Quantum Information: 10th Anniversary Edition*, 10th ed. (Cambridge University Press, New York, 2011).

[2] F. Arute, K. Arya, R. Babbush, D. Bacon, J. C. Bardin, R. Barends, R. Biswas, S. Boixo, F. G. S. L. Brandao, D. A. Buell, B. Burkett, Y. Chen, Z. Chen, B. Chiaro, R. Collins, W. Courtney, A. Dunsworth, E. Farhi, B. Foxen, A. Fowler, C. Gidney, M. Giustina, R. Graff, K. Guerin, S. Habegger, M. P. Harrigan, M. J. Hartmann, A. Ho, M. Hoffmann, T. Huang, T. S. Humble, S. V. Isakov, E. Jeffrey, Z. Jiang, D. Kafri, K. Kechedzhi, J. Kelly, P. V. Klimov, S. Knysh, A. Korotkov, F. Kostritsa, D. Landhuis, M. Lindmark, E. Lucero, D. Lyakh, S. Mandra, J. R. McClean, M. McEwen, A. Megrant, X. Mi, K. Michielsen, M. Mohseni, J. Mutus, O. Naaman, M. Neeley, C. Neill, M. Y. Niu, E. Ostby, A. Petukhov, J. C. Platt, C. Quintana, E. G. Rieffel, P. Roushan, N. C. Rubin, D. Sank, K. J. Satzinger, V. Smelyanskiy, K. J. Sung, M. D. Trevithick, A. Vainsencher, B. Villalonga, T. White, Z. J. Yao, P. Yeh, A. Zalcman, H. Neven, and J. M. Martinis, Quantum supremacy using a programmable superconducting processor, Nature (London) **574**, 505 (2019).

[3] S. McArdle, S. Endo, A. Aspuru-Guzik, S. C. Benjamin, and X. Yuan, Quantum computational chemistry, Rev. Mod. Phys. **92**, 015003 (2020).

[4] P. Jordan and E. Wigner, Über das paulische äquivalenzverbot, Z. Phys. **47**, 631 (1928).

[5] S. B. Bravyi and A. Y. Kitaev, Fermionic quantum computation, Ann. Phys. **298**, 210 (2002).

[6] A. Aspuru-Guzik, A. D. Dutoi, P. J. Love, and M. Head-Gordon, Simulated quantum computation of molecular energies, Science **309**, 1704 (2005).

[7] A. Peruzzo, J. McClean, P. Shadbolt, M.-H. Yung, X.-Q. Zhou, P. J. Love, A. Aspuru-Guzik, and J. L. O'Brien, A variational eigenvalue solver on a photonic quantum processor, Nat. Commun. **5**, 4213 (2014).

[8] P. J. J. O'Malley, R. Babbush, I. D. Kivlichan, J. Romero, J. R. McClean, R. Barends, J. Kelly, P. Roushan, A. Tranter, N. Ding, B. Campbell, Y. Chen, Z. Chen, B. Chiaro, A. Dunsworth, A. G. Fowler, E. Jeffrey, E. Lucero, A. Megrant, J. Y. Mutus, M. Neeley, C. Neill, C. Quintana, D. Sank, A. Vainsencher, J. Wenner, T. C. White, P. V. Coveney, P. J. Love, H. Neven, A. Aspuru-Guzik, and J. M. Martinis, Scalable Quantum Simulation of Molecular Energies, Phys. Rev. X **6**, 031007 (2016).

[9] A. Kandala, A. Mezzacapo, K. Temme, M. Takita, M. Brink, J. M. Chow, and J. M. Gambetta, Hardware-efficient variational quantum eigensolver for small molecules and quantum magnets, Nature (London) **549**, 242 (2017).

[10] C. Hempel, C. Maier, J. Romero, J. McClean, T. Monz, H. Shen, P. Jurcevic, B. P. Lanyon, P. Love, R. Babbush, A. Aspuru-Guzik, R. Blatt, and C. F. Roos, Quantum Chemistry Calculations on a Trapped-Ion Quantum Simulator, Phys. Rev. X **8**, 031022 (2018).

[11] J. R. McClean, M. E. Kimchi-Schwartz, J. Carter, and W. A. de Jong, Hybrid quantum-classical hierarchy for mitigation of decoherence and determination of excited states, Phys. Rev. A **95**, 042308 (2017).

[12] K. M. Nakanishi, K. Mitarai, and K. Fujii, Subspace-search variational quantum eigensolver for excited states, Phys. Rev. Research **1**, 033062 (2019).

[13] O. Higgott, D. Wang, and S. Brierley, Variational quantum computation of excited states, Quantum **3**, 156 (2019).

[14] R. Santagati, J. Wang, A. A. Gentile, S. Paesani, N. Wiebe, J. R. McClean, S. Morley-Short, P. J. Shadbolt, D. Bonneau, J. W. Silverstone, D. P. Tew, X. Zhou, J. L. O'Brien, and M. G. Thompson, Witnessing eigenstates for quantum simulation of Hamiltonian spectra, Sci. Adv. **4**, 9646 (2018).

[15] J. I. Colless, V. V. Ramasesh, D. Dahlen, M. S. Blok, M. E. Kimchi-Schwartz, J. R. McClean, J. Carter, W. A. de Jong, and I. Siddiqi, Computation of Molecular Spectra on a Quantum Processor with an Error-Resilient Algorithm, Phys. Rev. X **8**, 011021 (2018).

[16] T. Jones, S. Endo, S. McArdle, X. Yuan, and S. C. Benjamin, Variational quantum algorithms for discovering Hamiltonian spectra, Phys. Rev. A **99**, 062304 (2019).

[17] A. Damascelli, Probing the electronic structure of complex systems by ARPES, Phys. Scr. **2004**, 61 (2004).

[18] T. Kosugi and Y.-I. Matsushita, One-particle Green's function of interacting two electrons using analytic solutions for a three-body problem: Comparison with exact Kohn–Sham system, J. Phys.: Condens. Matter **30**, 435604 (2018).

[19] T. Kosugi and Y.-i. Matsushita, Construction of Green's functions on a quantum computer: Quasiparticle spectra of molecules, Phys. Rev. A **101**, 012330 (2020).
[20] D. Wecker, M. B. Hastings, N. Wiebe, B. K. Clark, C. Nayak, and M. Troyer, Solving strongly correlated electron models on a quantum computer, Phys. Rev. A **92**, 062318 (2015).
[21] B. Bauer, D. Wecker, A. J. Millis, M. B. Hastings, and M. Troyer, Hybrid Quantum-Classical Approach to Correlated Materials, Phys. Rev. X **6**, 031045 (2016).
[22] S. Endo, I. Kurata, and Y. O. Nakagawa, Calculation of the Green's function on near-term quantum computers, arXiv:1909.12250.
[23] G. Stefanucci and R. van Leeuwen, *Nonequilibrium Many-Body Theory of Quantum Systems* (Cambridge University Press, Cambridge, 2013).
[24] T. Kosugi and Y.-i. Matsushita, Quantum Singwi-Tosi-Land-Sjolander approach for interacting inhomogeneous systems under electromagnetic fields: Comparison with exact results, J. Chem. Phys. **147**, 114105 (2017).
[25] L. Hedin, New method for calculating the one-particle Green's function with application to the electron-gas problem, Phys. Rev. **139**, A796 (1965).
[26] A. D. McLean and M. Yoshimine, Theory of molecular polarizabilities, J. Chem. Phys. **47**, 1927 (1967).
[27] G. Maroulis, A complete description of the electric dipole moment, polarizability, and hyperpolarizability tensors of hydrogen peroxide, J. Chem. Phys. **96**, 6048 (1992).
[28] H. Hübener and F. Giustino, Time-dependent density functional theory using atomic orbitals and the self-consistent Sternheimer equation, Phys. Rev. B **89**, 085129 (2014).
[29] S. R. Elliott and M. Franz, Colloquium: Majorana fermions in nuclear, particle, and solid-state physics, Rev. Mod. Phys. **87**, 137 (2015).
[30] T. Helgaker, P. Jørgensen, and J. Olsen, *Molecular Electronic-Structure Theory* (Wiley, New York, 2000).
[31] J. T. Fermann and E. F. Valeev, Libint: Machine-generated library for efficient evaluation of molecular integrals over Gaussians (2003), freely available at http://libint.valeyev.net/ or one of the authors.
[32] R. Lehoucq, D. Sorensen, and C. Yang, *ARPACK Users' Guide* (Society for Industrial and Applied Mathematics, Philadelphia, 1998); http://epubs.siam.org/doi/pdf/10.1137/1.9780898719628.
[33] M. Douay, R. Nietmann, and P. Bernath, New observations of the A1πu-X1σg+ transition (Phillips system) of C_2, J. Mol. Spectrosc. **131**, 250 (1988).
[34] L. Bytautas and K. Ruedenberg, Correlation energy extrapolation by intrinsic scaling. iv. Accurate binding energies of the homonuclear diatomic molecules carbon, nitrogen, oxygen, and fluorine, J. Chem. Phys. **122**, 154110 (2005).
[35] K. Seki, T. Shirakawa, and S. Yunoki, Symmetry-adapted variational quantum eigensolver, Phys. Rev. A **101**, 052340 (2020).
[36] L. Sutton, *Tables of Interatomic Distances and Configuration in Molecules and Ions* (The Chemical Society, London, 1958).